Published in final edited form as:
J Immunol. 2013 April 15; 190(8): 4014–4026. doi:10.4049/jimmunol.1202963.

Bcl6 expressing follicular helper CD4 T cells are fate committed early and have the capacity to form memory

Youn Soo Choi[1], **Jessica A. Yang**[1], **Isharat Yusuf**[1], **Robert J. Johnston**[1,2], **Jason Greenbaum**[1], **Bjoern Peters**[1], and **Shane Crotty**[1,2,3,†]

[1]Division of Vaccine Discovery, La Jolla Institute for Allergy and Immunology, La Jolla, CA 92037

[2]Department of Medicine, University of California, San Diego School of Medicine, La Jolla, CA 92037

[3]Center for HIV/AIDS Vaccine Immunology and Immunogen Discovery, La Jolla, CA 92037

Abstract

Follicular helper CD4 T cells (Tfh) are a distinct type of differentiated CD4 T cells uniquely specialized for B cell help. Here we examined Tfh cell fate commitment, including distinguishing features of Tfh versus Th1 proliferation and survival. Using cell transfer approaches at early time points after an acute viral infection, we demonstrate that early Tfh cells and Th1 cells are already strongly cell fate committed by day three. Nevertheless, Tfh cell proliferation was tightly regulated in a TCR-dependent manner. The Tfh cells still depend on extrinsic cell fate cues from B cells in their physiological in vivo environment. Unexpectedly, we found that Tfh cells share a number of phenotypic parallels with memory precursor CD8 T cells, including selective upregulation of IL7Rα and a collection of co-regulated genes. As a consequence, the early Tfh cells can progress to robustly form memory cells. These data support the hypothesis that CD4 and CD8 T cells share core aspects of a memory cell precursor gene expression program involving Bcl6, and a strong relationship exists between Tfh cells and memory CD4 T cell development.

Keywords

Tfh cells; germinal center; LCMV infection; proliferation capacity; IL-7R; vaccine

Introduction

Follicular helper (Tfh) CD4 T cells are a subset of differentiated CD4 T cells that express CXCR5, the chemokine receptor for B cell homing chemokine CXCL13 (1). Surface CXCR5 expression enables Tfh cells to migrate into B cell follicles, where they provide help to B cells to form germinal centers (2). Tfh cells are required for generation of long-lived plasma cells and memory B cells through cognate interactions with germinal center B cells as well as production of B cell help cytokines such as IL-21 (3). Differentiation of effector CD4 T cell subsets is controlled by specific transcription factors (1, 4), and CD4 T cell differentiation into Tfh cells is regulated by the transcription factor Bcl6 (1). *Bcl6*-deficient CD4 T cells fail to differentiate into Tfh cells (5–7), whereas constitutive expression of Bcl6 instructs murine and human CD4 T cells to differentiate into Tfh cells (6, 8).

[†]Correspondence to: Shane Crotty, PhD, La Jolla Institute for Allergy and Immunology, 9420 Athena Circle, La Jolla, CA 92037, shane@liai.org, (858) 752-6816, (858) 752-6993 (fax).

Due to the importance of Bcl6 in Tfh cell differentiation, regulation of Bcl6 in CD4 T cells is of substantial interest. Several recent studies, including our own work, demonstrated that Bcl6 protein induction occurs quite early after CD4 T cells receive activation signals both in vivo (9–11) and in vitro (12–14). During the DC priming stage of CD4 T cells, ICOS is a key upstream molecule for induction of Bcl6 (9). In contrast, high expression of IL-2Rα and IL-2 dependent signaling through STAT5 severely limits Tfh differentiation (15). Tfh differentiation is augmented by reduced IL-2Rα gene copy number (IL-2Rα$^{+/-}$) or curtailed by exogenous IL-2 treatment (15, 16). Initial Bcl6 induction and subsequent CXCR5 expression leads CD4 T cells to the B-T border, where Tfh cells interact with cognate B cells to maintain Bcl6 expression for full differentiation and maintenance of the Tfh phenotype (1, 9, 11, 17).

Cells with Tfh and non-Tfh phenotypes are distinguishable from very early time points in vivo (9–11, 18). However, whether the early pathways for development of Tfh versus non-Tfh cells would be maintained in a given immune response remains an open issue. Very recently, Dong and colleagues reported that Tfh and Th2 cells remain their original phenotypes in recipient mice after rechallenge with antigen (19), indicating Tfh versus non-Tfh differentiation pathways are stable, but not inter-convertible. However, an earlier report demonstrated that Tfh cells can develop from IL-4 producing CXCR5^{-} CD4 T cells in recipient mice after antigen challenge (20). Indeed, it is well established from plasticity studies that many types of differentiated CD4 T cells can lose their differentiation program and acquire new differentiation programs (4, 12, 21–23). A recent study provided evidence of potential plasticity of Tfh cells in part by analysis of epigenetic modifications, which revealed positive regulatory H3K4me3 marks on major transcriptional regulators of Th1 (*Tbx21*), Th2 (*Gata3*), and Th17 (*Rorc*) cells, in ex vivo and in vitro generated Tfh cells (12). Furthermore, there are molecules capable of regulating both Tfh and Th1 cells. IL-12 mediated STAT4 activation has been associated with Bcl6 induction in CD4 T cells during Th1 differentiation, which presents a potential mechanism for plasticity between Tfh and Th1 cell differentiation (13, 14). Unexpectedly, excessive IFN-γ signaling augments Tfh differentiation in Sanroque mice, driving auto-antibody responses (24).

The transcriptional regulator Blimp1 is also involved in CD4 T cell differentiation, and is a key negative regulator of Tfh differentiation (6, 15). Through reciprocal regulations of Bcl6 and Blimp1, Tfh cell differentiation is distinguished from CD4 T cell differentiation into other differentiated cell types (Th1, Th2, Th17, and iTreg) (1, 6, 25, 26). Bcl6 can repress Blimp1 expression by directly binding to the *Prdm1* gene (encoding Blimp1) (27, 28). In B cells, Bcl6 is critically required for germinal center B cell differentiation and survival, while Blimp1 drives terminal differentiation of B cells into plasma cells (29, 30). Antagonistic regulation of Bcl6 and Blimp1 is also associated with molecular regulation of fate determination of CD8 T cells (31, 32). Recent studies demonstrated Tfh cells contribute to memory compartment of CD4 T cells (18, 19, 33). We therefore explored the regulation of Bcl6 and the stability of Tfh cell differentiation, and the potential relationship between Bcl6 expression of Tfh cells and memory CD4 T cell formation.

Using adoptive cell transfer experiments, we found that early Bcl6^{+}CXCR5^{+} Tfh cells exhibited substantial cell fate commitment and B cell help capacities. Gene expression profile analysis revealed that mature Tfh cells and early memory precursor CD8 T cells share a transcriptional signature, including Bcl6 expression and IL-7Rα re-expression. We demonstrate that Tfh cells contribute substantially to memory CD4 T cell generation after a viral infection, implying that aspects of Tfh differentiation and memory CD4 T cell development have shared mechanisms.

Materials and Methods

Mice and viral infections

C57BL/6J (B6), B cell-deficient μMT (C57BL/6J μ*MT*), and TCRα-deficient (B6.129S2-*Tcra*^{tm1Mom}/J) mice were purchased from the Jackson Laboratory. SMARTA ('SM'. LCMV gp66–77-IA^{b} specific) (34) and Blimp1-YFP BAC tg mice (35) were obtained from in-house breeders at LIAI. LCMV Armstrong strain was made and plaque forming units (PFUs) determined as previously described (36). All animal experiments were performed in compliance with approved animal protocols at LIAI. Whole-genome microsatellite analysis was conducted through the UCLA Southern California Genotyping Consortium. SM mice were greater than 99% B6.SJL *Ptprc*^{a}. All mice were housed in ventilated racks with HEPA filters and provided with irradiated PicoLab Rodent Diet (20–5053) food.

NP-OVA and gp61-KLH immunization

NP-OVA was prepared in alum and injected as previously described (6). Briefly, three parts of NP_{19}-OVA (Biosearch Technologies) in PBS was mixed with one part of Alum (Peirce) for 60 minutes at 4°C. 100 μg of NP-OVA-Alum immunizations were done intraperitoneally. gp61-KLH was prepared as follows. LCMV gP61 peptide (GLNGPDIYKGVYQFKSVEFD) was conjugated to malemide-activated KLH following the manufacturer's protocol (Pierce). 20 μg of GP61-KLH was resuspended in alum with 2 μg of LPS for intraperitoneal injections.

Retrovirus production and CD4 T cell transduction

Blimp1-expressing retroviral vector (pMIG-GFP) or empty vector (GFP only) were used to produce virions from the Plat-E cell line as previously described (6). Culture supernatants were obtained 2 days after transfections, and filtered through 0.45 μm syringe filters. CD4 T cells were negatively isolated by using CD4 T cell isolation kit (Miltenyi) for retroviral transductions as previously described (6). Briefly, cells were in vitro stimulated with 8 μg/ml of αCD3 (clone 17A2, BioXcell) and αCD28 (clone 37.51, BioXcell) and then transduced with retroviral virions 24 and 36 hours post stimulation. Transduced CD4 T cells were FACS sorted based on GFP expression levels.

Flow Cytometry

Single cell suspensions were obtained by a gentle mechanical disruption of spleens, followed by ACK lysis buffer to remove red blood cells. Cell suspensions were stained with the following monoclonal antibodies in FACS buffer (PBS with 0.5% BSA): CD4, CD8, Bcl6, CXCR5, pSTAT5 (BD Biosciences); SLAM (CD150, Biolegend); CD200, CD44, CD45.1/2, IL-2Rα (CD25), IL-7Rα (CD127), CD62L, CD69, B220, BTLA, IFN-γ (eBioscience).

CXCR5 stains were performed as previously described (6, 9). For early time point analysis (day 2 and 3 after LCMV infection), biotinylated CXCR5 (BD Biosciences) was used. Briefly, cells were stained with biotinylated CXCR5 mAb in FACS buffer for 30 minutes at 4°C, washed with FACS buffer twice, followed by secondary step stains with streptavidin-PE (PE Cy7, or APC) (eBiosciences) and mAbs for other surface molecules of interest. For later time point analysis, the tertiary CXCR5 stain was used. Briefly, cells were stained with purified αCXCR5 mAb (BD Biosciences) for 1 hour at 4°C, washed with FACS buffer twice, and stained with secondary biotinylated goat anti-rat Ig(H+L) (Jackson Immunoresearch) for 30 minutes at 4°C. After two washes with FACS buffer, tertiary staining was performed with streptavidin-PE (PE Cy7, or APC) (eBiosciences) and other mAbs for surface molecules of interest. Primary and secondary stains were done in PBS + 0.5% BSA + 2% FCS + 2% Normal Mouse Serum.

Intracellular Bcl6 (K112-91) was performed using Foxp3 staining buffers (eBioscience). The cells were fixed (30 minutes to 1 hour) at 4°C and then washed twice with 1X permeabilization buffer. Anti-Bcl6 mAbs were diluted in 1X permeabilization buffer and applied to fixed samples (30 minutes to 1 hour) at 4°C.

For intracellular IFN-γ stain, splenocytes were stimulated with PMA (20 ng/ml) and Ionomycin (1μM) for 4 hours in the presence of brefeldin A. Intracellular IFN-γ was detected as previously described (6).

All FACS samples were washed twice with FACS buffer and either acquired using an LSRII (BD Biosciences) or sorted by FACS Aria (BD Biosciences). Data were analyzed using FlowJo (Tree Star).

CellTrace Violet label

Cell suspensions were washed and resuspended in PBS at 10^7 cells/ml concentration. CellTrace Violet (Invitrogen) at a final concentration 2.5 μM was and incubated with cells for 20 minutes at 37°C, protected from light. Unlabeled CellTrace Violet was then quenched by adding 2 to 5 times volume of FBS to the original staining volume of cell suspensions, spun, and resuspended in appropriate media.

Cell transfer and in vitro culture

Naïve SM CD4 T cells were purified from whole splenocytes by negative selection using magnetic beads (Miltenyi). Naïve SM or retrovirally transduced OTII CD4 T cells were transferred into recipient mice by intravenous injections via the retro-orbital sinus. Cell transfer numbers for each time point were as follows: For naïve SM cells, 1×10^6, $4–5 \times 10^5$, and 5×10^3 SM $CD4^+$ T cells for day 2, 3, and 8 experiments, respectively. 2.5×10^3 transduced OTII CD4 T cells were transferred for analysis of OTII CD4 T cells 8 days after NP-OVA protein immunization. For adoptive transfers of sorted cells in the fate commitment and memory analysis, two groups of infection-matched B6 or $TCR\alpha^{-/-}$ mice were injected with the same numbers of Tfh and Th1 SM cells (range of $50 – 100 \times 10^3$). DMEM was used for all adoptive cell transfer procedure.

For in vitro cultures of Tfh and Th1 SM cells, 96-well flat bottom plates were pre-coated with 8 μg/ml of αCD3 and αCD28, unless the amount of αCD28 mAb was specified in Figure Legends. Cells were resuspended in the complete culture media (DMEM + 10% FCS (fetal calf serum), supplemented with 2mM GlutaMAX (Gibco), 100 U/mL Penicillin/ Streptomycin (Gibco), and 50 μM BME), and 2 ng/ml rh IL-7 (Peprotech).

Microarray meta-analysis

Datasets—All CEL files were downloaded from the NCBI GEO database (GSE19825, GSE21379-GSE21381).

Data normalization and summarization—Data from three separate studies were analyzed in this analysis. Microarrays were background-corrected and normalized using the ‘rma’ function of the Bioconductor ‘affy’ package (37). Data from each study were normalized separately. Within each study, each possible comparison of Th1 vs. Tfh and CD8 effector vs. CD8 memory precursors was performed. Genes that had an average 2-fold difference across all comparisons are included in Supplementary Table 1. A heatmap for selected genes of interest was generated using matrix2png (38) and shown in Figure 5B.

Statistics

Statistical analyses were done using Prism 5.0 (GraphPad) and P-values were obtained by using two-tailed unpaired Student's t tests with a 95% confidence interval. Error bars on bar graphs depict the standard error of mean (SEM). For statistical analysis of microarray data, a contingency table of genes that were up- or down-regulated in both the Th1 vs. Tfh CD4 T cells and effector vs. memory precursors CD8 T cells comparisons was produced (Supplementary Table 1) and used to calculate P value of 1.0×10^{-14} with a Fisher's exact test.

Results

Early Tfh versus Th1 bifurcation after acute viral infection

$Bcl6^{+}CXCR5^{+}$ Tfh cells are generated early during the DC priming stage of immune responses (9–11, 39). Careful analysis of Bcl6 protein expression during the early phase of CD4 T cell activation confirmed that Bcl6 is specifically induced early in Tfh cells (Figure 1A–B. Supplemental Figure 1). At the same time points after LCMV infection, $Bcl6^{-}CXCR5^{-}$ non-Tfh cells are also identifiable and were shown to strongly express IL-2Rα, the high affinity IL-2R subunit, and Blimp1, as measured with a Blimp1-YFP reporter (9, 18). We then established that the non-Tfh SM cells were Th1 cells. Day 3 $IL\text{-}2R\alpha^{+}Blimp1_{YFP}^{+}$ non-Tfh and $IL\text{-}2R\alpha^{-}$ $Blimp1_{YFP}^{-}$ Tfh cells were sorted for qPCR analysis. Tbx21 mRNA (encoding T-bet) was expressed 10-fold higher in $IL\text{-}2R\alpha^{+}Blimp1_{YFP}^{+}$ cells compared to $IL\text{-}2R\alpha^{-}Blimp1_{YFP}^{-}$ Tfh cells (Figure 1C. $p = 2.5 \times 10^{-6}$). T-bet protein was strongly expressed in $IL\text{-}2R\alpha^{+}Blimp1_{YFP}^{+}$ cells (Figure 1D. $p = 0.0004$). $IL\text{-}2R\alpha^{+}$ cells were the major population in IFN-γ production at day 3 after LCMV infection (Figure 1E. $p = 2.3 \times 10^{-5}$). Thus, the early Tfh cells are $CXCR5^{+}IL\text{-}2R\alpha^{int/-}Blimp1_{YFP}^{-}$, and the $T\text{-}bet^{hi}IL\text{-}2R\alpha^{+}Blimp1_{YFP}^{+}$ cells are Th1 cells.

Cell fate commitment of early Tfh and Th1 cells

Different models have been put forward as to whether Tfh differentiation is an independent pathway or a subsequent state of other effector CD4 T cells (1, 9, 40). Therefore, we explored whether early $Bcl6^{+}CXCR5^{+}$ CD4 T cells are cell fate committed. To address whether early Tfh and Th1 cells interconvert, we sorted Tfh and Th1 cells from "donor" B6 mice 3 days after LCMV infection for transfers into recipient mice (Figure 2A). SM cells were sorted as either $IL\text{-}2R\alpha^{+}Blimp1_{YFP}^{+}$ ($Bcl6^{-}CXCR5^{-}$) Th1 cells or $IL\text{-}2R\alpha^{-}Blimp1_{YFP}^{-}$ ($Bcl6^{+}CXCR5^{+}$) Tfh cells (Figure 2A–C), and then transferred into separate groups of infection-matched B6 recipients, to provide the same physiological environment (Figure 2A). Eight days after LCMV infection (five days after transfers), we examined Tfh and Th1 cell recipient mice to analyze the stability of Tfh and Th1 cell populations in each recipient group. Quite strikingly, we found that Tfh and Th1 cells maintained their original phenotypes (Figure 2D). The vast majority of input Tfh cells remained $SLAM^{lo}CXCR5^{+}$ Tfh cells (80 – 92%, Figure 2D–E. $p = 2.7 \times 10^{-10}$). The majority of input Th1 cells retained their phenotype and did not convert to Tfh cells (80 – 87%, Figure 2D–E. $p = 1.4 \times 10^{-9}$). High levels of Bcl6 were maintained by transferred Tfh SM cells (Figure 2F. $p = 5.9 \times 10^{-6}$), whereas $Blimp1_{YFP}$ was highly expressed by SM cells in Th1 recipients B6 mice (Figure 2G. $p = 3.7 \times 10^{-10}$). Tfh cells are distinguished from other effector CD4 T cells, by their prominent roles in providing B cell help (1). Hence, we addressed whether day 3 Tfh cells were capable of B cell help. Day 3 Tfh and Th1 cells were isolated from LCMV infected donor B6 mice and then transferred into $TCR\alpha^{-/-}$ mice that were immunized with gp61-KLH. Day 3 Tfh cells were able to induce germinal center B cells in $TCR\alpha^{-/-}$ mice (Figure 2H. $p = 2.7 \times 10^{-3}$), which was associated with a robust formation of $Bcl6^{+}CXCR5^{+}$ Tfh cells (Figure 2I. $p = 1.0 \times 10^{-5}$). These results demonstrate

that Tfh and Th1 cells are predominantly fate committed within 72 hours of responding to an acute infection, both by transcription factor expression and cell function.

Early Tfh cells require antigen presentation for every round of cell division

When we analyzed Tfh and Th1 cell recipient B6 mice, we observed that SM cell recoveries from Tfh cell recipients were 5 to 10-fold more than from Th1 cell recipients (Figure 3A. $p = 6.3 \times 10^{-5}$). Comparable levels of activation of endogenous CD4 and CD8 T cells excluded the possibility of different levels of LCMV infection (data not shown). We therefore examined whether early Tfh cells have different proliferative capacity than Th1 cells. To address this point, Tfh cells (IL-2Rα^{-}Blimp1$_{YFP}^{-}$) and Th1 cells (IL-2Rα^{+}Blimp1$_{YFP}^{+}$) were sorted from B6 mice 3 days after LCMV infection as described in Figure 2A, labeled with a proliferation tracking dye, and then transferred into infection-matched B6 mice. Five days after transfers, both Tfh and Th1 cells had fully diluted the proliferation tracking dye (Figure 3B), which indicated that both cell types proliferated extensively (≥ 10 divisions).

We next investigated the proliferation capacities of Tfh and Th1 cells in a defined in vitro environment. For this, Tfh and Th1 SM cells were sorted from LCMV infected mice three days after infection (Figure 2A) and cultured in the presence or absence of TCR- and costimulation-mediated activation (αCD3/CD28 mAbs) (Figure 3C–D). In the presence of stimulation, Th1 cells proliferated more than Tfh cells (Figure 3C. $p = 6.3 \times 10^{-6}$). Interestingly, we also found that Th1 cells underwent several rounds of cell division in the absence of antigenic stimulation, which was in marked contrast to Tfh cells that underwent no proliferation in the absence of TCR-mediated stimulation (Figure 3D. $p = 5.9 \times 10^{-6}$).

TCR stimulation leads to upregulation of IL-2Rα on T cells (41). This results in a possible conundrum during the expansion phase of the CD4 T cell response, where repeated TCR stimulation is strictly required for Tfh cell proliferation but also results in antagonism of Bcl6 by upregulation of IL-2Rα and Blimp1 (9, 15). We therefore examined the regulation of these proteins in early Tfh and Th1 cells during proliferation. Day 3 Tfh cells do not express IL-2Rα or Blimp1$_{YFP}$ (Figure 3E–F), but Tfh cells nevertheless require TCR stimulation for continued expansion. Interestingly, TCR stimulation of Tfh cells did not induce IL-2Rα expression, in contrast to robust upregulation of IL-2Rα on Th1 cells in vitro after TCR stimulation (Figure 3E, right panel. $p = 7.6 \times 10^{-11}$). We infer that avoidance of IL-2Rα induction is important for Tfh cell maintenance, as upregulation of IL-2Rα on Th1 cells after TCR stimulation was associated with a 10-fold further induction of Blimp1$_{YFP}$ (Figure 3F). Therefore, proliferating Tfh cells dissociate TCR signaling from IL-2Rα expression.

A series of studies has demonstrated that antigen presentation first by DCs during the CD4 T cell priming stage followed by antigen presentation by B cells is a prerequisite for CD4 T cells to initiate and then complete Tfh differentiation (2, 6, 9, 42–45). The strict antigen dependence of Tfh cell proliferation made us investigate whether antigen presentation in vivo may affect cell fate commitment in Tfh cells. For this, fate committed Tfh cells were sorted from LCMV infected mice at day 3 after infection and transferred into infection-matched B6 and B cell-deficient μMT mice. Within the normal physiological environment (B6 mice), fate committed Tfh cells (Bcl6^{+}CXCR5^{+}) again maintained their phenotype as Tfh cells (Figure 3G). However, transferred Tfh cells were lost in the absence of B cells. Indeed in Tfh cell recipient μMT mice, Blimp1$_{YFP}$ expressing Th1 cells (SLAM^{hi}CXCR5^{-}) were highly enriched 5 days after cell transfers (15 ± 2 % in B6 vs. 43 ± 8 % in μMT) (Figure 3G–H). Our data indicates that B cells are important APCs for Tfh cells not only for maintenance of Bcl6 expression (9) (Figure 3I) but also for each round of cell proliferation (Figure 3D).

Fate committed Tfh cells share a molecular signature with CD8 T memory precursors

Our data indicate that the fate committed differentiation of early bifurcated Tfh versus Th1 cells is strongly associated with reciprocal regulation of Bcl6 and Blimp1. Interestingly, antagonistic Bcl6 – Blimp1 signaling axis is also observed during the antigen specific CD8 T cell differentiation; $Bcl6^+$ memory precursor CD8 T cells and $Blimp1^+$ short-lived effector CD8 T cells are present at the peak response to LCMV infection (46). The gene expression pattern of these two CD8 T cell populations has been characterized (35). Memory precursor CD8 T cells express elevated levels of Bcl6, whereas terminal effector CD8 T cells express elevated levels of Blimp1, which led us to investigate whether Bcl6 expressing Tfh versus $Blimp1^+$ Th1 cells may possess similar molecular regulation to memory precursor versus effector precursor CD8 T cells. Given that memory precursor CD4 T cells were recently proposed to be present in a $PSGL1^{hi}Ly6C^{lo}$ population (47), we examined whether Bcl6 and Blimp1 based phenotyping is recapitulated by phenotypic analysis of CD4 T cells based on PSGL1 and Ly6C. At day 8 after LCMV infection, Blimp1-YFP reporter SM (Figure 4A–D) and polyclonal (Figure 4E–F) CD4 T cells were analyzed based on PSGL1 and Ly6C. Our data is consistent with a previous study (47), where $PSGL1^{hi}Ly6C^{hi}$ and $PSGL1^{lo}Ly6C^{lo}$ exhibited strong expression of $Blimp1_{YFP}$ and Bcl6, respectively (Figure 4C–D). However, we found that both $Blimp1_{YFP}{}^{-}CXCR5^{+}(Bcl6^{+})$ Tfh and $Blimp1_{YFP}{}^{+}CXCR5^{-}(Bcl6^{-})$ Th1 cells were mixed in the $PSGL1^{hi}Ly6C^{lo}$ gate (Figure 4A–B and 4E–F).

Memory precursor CD8 T cells have been distinguished as early as 3.5 days in vivo after LCMV infection, on the basis of IL-2Rα expression (48), and differential IL-2 signaling can preferentially direct activated CD8 T cells to short-lived effector ($perforin^{hi}Blimp1^{+}$) or memory cell precursor ($IL\text{-}7R\alpha^{+}Bcl6^{+}$) fates (49). Given that differential IL-2Rα expression on early memory precursor CD8 T cells versus terminal effector biased CD8 T cells parallels differential IL-2Rα expression on early Tfh cells versus Th1 cells (9) (Figure 2), we took an unbiased approach to ask whether Tfh differentiation pathway may share a molecular program with early memory precursor CD8 T cells, identifiable as a transcriptional signature. Gene expression data for day 3.5 memory precursor and effector-biased CD8 T cells populations was compared to gene expression data for day 8 Tfh and Th1 CD4 T cell populations. The full data sets were queried for the set of all genes differentially expressed (≥ 2-fold) by Tfh cells compared to Th1 cells, and also differentially expressed by early memory precursor CD8 T cells compared to short-lived effector biased CD8 T cells. This screening was done irrespective of the directionality of the gene expression changes in each data set. 173 gene transcripts satisfied these conditions (Supplementary Table 1). Impressively, of the 173 gene expression changes, 95 genes were upregulated in both Tfh cells and memory precursor CD8 T cells, and 45 genes were downregulated in both Tfh cells and memory precursor CD8 T cells (Figure 5A and Supplemental Table 1). This gave a cumulative total of 140 out of 173 gene expression changes being in a shared direction in Tfh cells and memory precursor CD8 T cells. Only a small number of genes did not exhibit shared directionality. This was a highly nonrandom distribution of shared directionality ($p = 1.0 \times 10^{-14}$), indicating the presence of a shared gene expression program between Tfh cells and memory precursor CD8 T cells. Bcl6 and Blimp1 both appear in this gene set, in addition to many other genes with known or potential connections to memory cell development (Figure 5B).

These “memory type” gene expression patterns were then tested for their ability to predict early gene expression differences in day 3 Tfh versus Th1 cells. RNA was isolated from sorted day 3 Tfh and Th1 cells (Figure 2A) and analyzed for specific gene expression differences. Bcl6 and Blimp1 were confirmed to be strongly differentially expressed between early Tfh and Th1 cells (40-fold *Bcl6* mRNA difference, $p = 1 \times 10^{-6}$.51-fold *Prdm1* difference, $p = 9.2 \times 10^{-5}$. Figure 5C). In addition to *Bcl6*, the early fate committed Tfh cells induced strong expression of genes that were also highly upregulated by memory

precursors CD8 T cells (48), including *Tcf7* (38-fold, $p = 1 \times 10^{-6}$) (50), *Tox2* (14-fold, $p = 5 \times 10^{-6}$), and *Id3* (96-fold, $p = 2 \times 10^{-6}$) (51) (Figure 5D). Interestingly, several cell surface receptors strongly associated with Tfh cell functions were unexpectedly predicted to be associated with memory programming (Figure 5F), and indeed had strong expression differences between early Tfh and Th1 cells, including *Cd200* (11-fold, $p = 1.61 \times 10^{-6}$), *Btla* (5-fold, $p = 5.46 \times 10^{-6}$), and *Ly108* (3-fold, p = 0.008) (Figure 5E). In contrast, genes that were strongly suppressed by memory precursor CD8 T cells, such as *Id2, Havcr2,* and *Il2ra,* were substantially downregulated by the early fate committed Tfh cells compared to Th1 cell counterparts (Figure 5G) (35, 48, 49, 52). Each predicted gene expression change tested was correct. This is consistent with the presence of an underlying gene expression profile linking part of Tfh cell biology with the generation of T cell memory.

Development of memory CD4 T cells

The findings regarding Tfh cell fate commitment and shared gene expression with memory precursor CD8 T cells led us to examine whether early differentiated Tfh cells may contribute to the CD4 T cell memory compartment after an acute viral infection. We transferred day 3 $CD45.1^+$ Tfh and Th1 SM cells into infection matched $CD45.2^+$ recipients, which were then analyzed at immune memory time points (day 30 – day 45 post infection) (Figure 6A). Strikingly, at memory time points we found significantly more SM cells in early Tfh recipient mice than in mice that received early Th1 cells (Figure 6B. p = 0.015 at day 45) (p = 0.0007 at day 30, data not shown). Furthermore, the vast majority of transferred Tfh cells were found as $CXCR5^+$ Tfh cells (Figure 6B. 85 ± 2 % and 78 ± 5 % of total transferred cells at day 30 and 45 p.i. respectively). In sharp contrast, early Th1 cells failed to maintain their phenotype and were identified as three populations: $Blimp1_{YFP}{}^+CXCR5^-$, $Blimp1_{YFP}{}^-$ $CXCR5^-$, and $Blimp1_{YFP}{}^-$ $CXCR5^+$ (Figure 6B). Early Tfh cell recipient mice had a small but significant increase in Bcl6 expression compared to Th1 cell recipient mice (Figure 6C). Taken together, our data demonstrates that large numbers of memory CD4 T cells are derived from the early Tfh cell population and long-term survival of these cells is associated with Bcl6 expression.

Long-term survival of Tfh cells is associated with re-expression of IL-7Rα during the late, but not early, Tfh differentiation program

Our data implied that Tfh cells acquired cell intrinsic survival program during differentiation and thus could remain at higher frequencies at memory points (Figure 6). IL-7 signaling through IL-7Rα is critical for long-term survival of memory CD4 T cells. A lack of either IL-7 or IL-7Rα expression leads to defective development and maintenance of memory CD4 T cells (53, 54). Surface IL-7Rα expression is also associated with long-term survival of memory CD8 T cells (46). Therefore we investigated the expression levels of IL-7Rα on memory Tfh cells ($CXCR5^+Blimp1_{YFP}{}^-$) and Th1 cells ($CXCR5^-Blimp1_{YFP}{}^+$) in respective recipient mice. Both Tfh and Th1 memory cells expressed higher levels of IL-7Rα than naïve CD4 T cells ($CD44^{lo}$) (Figure 7A). Interestingly, IL-7Rα was statistically higher on memory Tfh cells than Th1 cells (Figure 7A. p = 0.02). We then examined whether differences in IL-7Rα expression in Tfh cells occur early during the immune responses. At 3 days after LCMV infection, IL-7Rα was strongly downregulated by both Tfh and Th1 cells (Figure 7B). Strikingly, at day 8, the peak of the CD4 response to LCMV infection, we found that IL-7Rα was selectively re-expressed by a fraction of $CXCR5^+$ CD4 T cells (20 ± 2 % $IL7R\alpha^+$ Tfh. $p = 4.4 \times 10^{-5}$ for Tfh vs. Th1) (Figure 7C–D). IL-7Rα re-expression on Tfh cells became even more dramatic 11 days after infection. More than 75% of Tfh cells regained IL-7Rα expression ($p = 2.8 \times 10^{-6}$ for Tfh vs. Th1) (Figure 7E–F). Taken together, our data demonstrates that Tfh cells exhibit superior re-expression of IL-7Rα to Th1 cells during the late stages of an LCMV infection, and it is associated with a survival advantage of Tfh cells at memory time points of the immune response to LCMV infection (Figure 6A).

Proliferation responsiveness of mature Tfh cells

Abundance of memory cells after early Tfh cell transfers compared to early Th1 cell transfers as well as selective re-expression of IL-7Rα of mature Tfh cells led us to examine the proliferation capacity of fully differentiated Tfh cells in greater detail. To address this point, we sorted Tfh cells (PD-1^{hi}CXCR5^{+}Blimp1_{YFP}^{-}) and Th1 cells (PD-1^{int}CXCR5^{-}Blimp1_{YFP}^{+}) at day 8 after LCMV infection, the peak of the CD4 T cell response (Figure 8A–B). The cells were then labeled with a proliferation tracking dye and cultured in the presence or absence of αCD3/28 mAbs. In the absence of antigenic stimulation signals, neither day 8 Th1 or Tfh cells proliferated in vitro (Figure 8C. Gray filled histograms). However, once TCR and costimulation signals were provided, Tfh cells proliferated well (Figure 8C. Colored lines), whereas Th1 cells proliferated poorly (Figure 8C, bar graph. $p = 4.0 \times 10^{-6}$, 4.3×10^{-6}, and 4.8×10^{-7} for 8, 2, and 0.5 μg/ml of αCD28 respectively). This was quite different from the early Th1 cells, which proliferated vigorously even in the absence of TCR signals (Figure 3D). Interestingly, while Tfh cells required TCR stimulation for proliferation at day 8, we found that costimulatory signaling via CD28 was minimally involved (48 ± 1 % and 33 ± 0.8 % proliferations by 8 and 0.5 μg/ml of αCD28, respectively. Figure 8C). We speculated that early TCR signaling may be altered in fully differentiated Th1 effector cells such that glycolytic metabolism was limited, preventing proliferation. We therefore examined Th1 cell blasting following TCR stimulation. Th1 cells robustly increased cell size in response to TCR signals (Figure 8D. $p = 7.5 \times 10^{-5}$), indicating that the block in Th1 proliferation was far downstream of TCR signaling and glycolytic metabolism. We therefore investigated whether different proliferation capacities of Tfh and Th1 cells were associated with Blimp1 expression, a highly anti-proliferative molecule (55). Th1 cells expressed $Blimp1_{YFP}$ at 15-fold higher levels than Tfh cells (Figure 8E. $p = 5.3 \times 10^{-8}$, no stim). After 72 hours of restimulation, while only a small fraction of Tfh cells could express $Blimp1_{YFP}$, Th1 cells further increased $Blimp1_{YFP}$ expression (Figure 8E–F). Moreover, in vivo experiments demonstrated that high expression of Blimp1 blocks CD4 T cell proliferation. Ova-specific TCRtg (OTII) CD4 T cells transduced with a Blimp1 expressing retroviral expression vector (Blimp1-GFP) exhibited significantly less proliferation in vivo at day 8 after NP-Ova immunization when the OTII CD4 T cells expressed high levels of Blimp1 versus intermediate levels of Blimp1 (Figure 8G–H. Blimp1^{int} vs. Blimp1^{hi}, p = 0.002). In summary, the capacity of mature Tfh cells to respond to TCR-mediated activation signals at the peak of the immune response was associated with more Tfh cells being found at memory time points after LCMV infection (Figure 6A), possibly due to proliferation induced by antigen presentation by germinal center B cells and the lack of Blimp1 expression by Tfh cells. Taken together, these data show that Bcl6^{+}CXCR5^{+} Tfh cells become fate committed early after an acute viral infection, and acquire distinct proliferation and survival capacities compared to Th1 cells.

Discussion

The stability of Tfh cells and the stability of Bcl6 expression in Tfh cells have been questions of great interest (56), accentuated by recent findings of plasticity of many types of differentiated CD4 T cells (21, 57, 58). Recent work has revealed plasticity of Tfh cells (12–14, 59). Conversion of transferred Tfh cells into Th1 cells was observed during a recall response to influenza virus infection in recipient mice (59). However, similar conversions have been reported by both in vitro and in vivo activated Th1, Th2, iTreg, and Th17 cells for reprogramming to other Th differentiation program (23, 60, 61). There are numerous examples that if the external forces are strong enough, then differentiated CD4 T cells can change their differentiation programming to respond to new environmental cues, even including extreme events such as Th2 cells acquiring Th1 differentiation in vivo (62). As

such, it is unclear whether Tfh cells possess any more plasticity than other CD4 T cell differentiation programs. Therefore, we focused on cell fate commitment within physiological environment. As described here, we found that early differentiated Tfh (or Th1) cells maintained their original differentiation pathway in recipient mice during the course of LCMV infection, and hence were cell fate committed. Our data is consistent with a recent study, which demonstrates transferred Tfh and Th2 cells remained stable in recipient mice upon antigen challenge (19). Therefore, our data support the concept that Tfh cells primarily develop as an independent differentiation pathway, starting from the earliest stages of DC priming (9, 40). However, this does not rule out the possibility that there are multiple pathways to Tfh cell differentiation and that differentiated cells may convert to Tfh cells under strong environmental cues (20, 63).

Similar to stem cells (64) and a variety of cell types studied in the context of developmental biology where non-cell autonomous positional cues and microanatomical niches are a central attribute of cell fate determination, maintenance of Tfh cell fate commitment differentiation is dependent on external factors. Tfh cells are lost if forced into a nonphysiological environment (Figure 3). The extrinsic signals provided by B cells include antigen presentation, ICOSL, and possibly other Tfh cell maintenance factors. These signals are critical for Tfh cells to maintain a high Bcl6 to T-bet ratio. Lack of those external signals in μMT mice (2, 6, 9, 44) or in mice where ICOS-ICOSL interaction is specifically blocked during cognate B:T interaction (9, 40) leads to reduced expression of Bcl6. Bcl6 can repress T-bet (7). Proinflammatory cytokines in LCMV infected animals may continuously drive T-bet expression. Hence, a concomitant inverted Bcl6 to T-bet ratio (Bcl6<T-bet) is observed in Tfh cells of μMT mice (data not shown), which putatively leads to the DNA-binding domain of Bcl6 being masked by T-bet (65), causing a loss of Bcl6-mediated Blimp1 repression. As a result, $CXCR5^+$ Tfh cells in Tfh recipient μMT mice expressed Blimp1 at a much higher level compared to Tfh cells in B6 mice (Figure 2).

The rigid requirement of antigen presentation, initially by DCs and followed by B cells, is one of the unique features for Tfh differentiation (2, 6, 9, 40, 42, 43). Relatively short TCR stimulation is sufficient for CD8 T cells to proliferate and differentiate into effector cells (66, 67). In sharp contrast, CD4 T cells are highly dependent on antigen recognition to continue proliferation and complete their differentiation (68). Our in vitro experiments with ex vivo Tfh versus Th1 cells from day 3 LCMV infected animals clearly show that Tfh cells require antigen presentation for each round of cell division. Notably, Tfh cells obtained at the peak response to LCMV infection proliferated upon TCR stimulation, whereas Th1 cells did not; therefore, Tfh differentiation program could be biased toward development of memory CD4 T cells that maintain TCR-mediated proliferative capacity. Along with previous work that demonstrated generation of memory CD4 T cells by $CXCR5^+$ CD4 T cells (18, 19, 33, 59), the present study indicates early Tfh differentiation pathway shares properties with memory CD4 T cells. However, we do not agree with the conclusion that the $CXCR5^+$ cells were not Tfh cells (18). That conclusion was based on a lack of short term co-localization with B cells, but that cell transfer was restricted to only a subfraction of the $CXCR5^+PD1^{lo}$ population that were also highly expressing CCR7 (18). Contrary to that conclusion, the $CXCR5^+PD1^{lo}$ cells were dependent on B cells for their development, indicating the CXCR5 expression was functional for co-localizing with B cells (18). The majority of day 8 $CXCR5^+$ CD4 T cells localize to B cell follicle and T/B border in independent studies (33, 69). Our data demonstrate that the vast majority of all $CXCR5^+$ CD4 T cells in a viral infection develop from a $Bcl6^+CXCR5^+$ early Tfh cell population.

Bcl6 has been previously implicated in memory T cell development, particularly memory CD8 T cell development (32, 35, 54). By cell transfer experiments, we showed that antigen-experienced CD4 T cells rapidly acquired preferential cell fates associated with differential

Bcl6 and Blimp1 expression. Our data here indicate that some functions of the Bcl6 - Blimp1 regulatory axis are shared in CD4 T cells and CD8 T cells and control a gene expression program regulating memory formation. Preferential re-expression of IL-7Rα by Bcl6-expressing Tfh cells (Figure 7) was a striking indication that this relationship was deeper than it first appeared. Our data also show that Tfh cells retained an enhanced capacity to respond to TCR stimulation compared to Th1 cells. This parallels observations for memory precursor CD8 T cells (35). These relationships between Tfh cell biology and memory T cell biology appear to repeatedly center on the Bcl6 – Blimp1 signaling axis. Notably, Tfh cells were lost in the absence of B cells, in agreement with previous observations of B cell dependent memory CD4 T cell development (70), providing another connection between Bcl6, Tfh cells, and CD4 T cell memory. Meta-analysis of Tfh cell and memory precursor CD8 T cell gene expression revealed potential genes that may form a transcriptional regulatory network with Bcl6 to facilitate memory T cell formation (Figure 5). *Tcf-7*, which encodes Tcf-1, is a downstream effector of the wnt signaling pathway and was shown to be required for CD8 T cell central memory development (50, 71). However, data of Prlic and Bevan argues against the requirement of wnt signaling in memory T cell formation since they observed a normal memory formation in T cell specific β-catenin deficient mice (72). Further investigation is required to address whether memory formation of T cells could be regulated by β-catenin independent activation of Tcf-1. Id proteins partner with E proteins to modulate a wide range of lymphocyte differentiation processes (73), and Id proteins appear to have partially overlapping and partially distinct functions. *Id2*-deficient CD8 T cells failed to differentiate into effector CD8 T cells, whereas *Id2*-deficient memory precursor CD8 T cell development was relatively intact (52, 74–76). Recent data suggests that Id proteins have important but complex roles in CD4 T cell fates (51). Collectively, our data indicate that CD4 and CD8 T cells share a common molecular signature involving Bcl6 for development of memory precursor cells.

Given these findings, it is of interest to understand how Bcl6 facilitates memory T cell formation. Our data indicates IL-7Rα is somehow involved, and IL-7Rα has an important role in long-term survival of memory CD4 T cells (46, 53, 77). Selective IL-7Rα expression identifies memory precursor CD8 T cells (46). Even though IL-7Rα expression alone is not sufficient for identifying memory precursor of CD4 T cells (47), here we show that IL-7Rα expression was preferentially regained by Tfh cells. All available data indicate that Bcl6 is an obligatory transcriptional repressor (78, 79), suggesting that preferential upregulation of IL-7Rα is not due to direct activity of Bcl6 at the *Il7Ra* gene, but it could be due to Bcl6 mediated repression of an intermediary transcriptional repressor, such as Blimp-1 (35). In addition, these different CD4 T cell fates were associated with differential IL-2Rα expression early. A similar process is seen with early differentiating CD8 T cells (48, 49). It is striking that IL-2R and IL-7R repeatedly appear in opposition when comparing T cell populations, with IL-2R favoring terminal effector T cell differentiation and IL-7R expression favoring memory T cell development.

Vaccines are predicated on the existence of immunological memory. Memory T cells develop from a fraction of the activated T cells that survive long term and can undergo recall responses to the same antigen (80–82). Recent human studies support the conclusion that $CXCR5^+CD45RO^+$ CD4 T cells are functional memory Tfh cells (83). Human genetic data also supports this conclusion, as rare individuals with *Icos* gene deletions specifically lack $CXCR5^+CD45RO^+$ CD4 T cells (84), and ICOS is required for Tfh cell differentiation (9, 40). Here we found that day 3 $Bcl6^+CXCR5^+$ Tfh cells are precursors of memory Tfh cells. Given that memory T cells are important for many developing vaccine strategies, and Tfh cell function is likely essential for virtually all humoral immunity based vaccine strategies, regulation of Bcl6 in T cells has promise for providing key insights into understanding molecular regulation of both Tfh cell development and memory T cell formation.

Supplementary Material

Refer to Web version on PubMed Central for supplementary material.

Acknowledgments

This work was supported by NIH NIAID grants (R01 072543 and R01 063107), Scripps CHAVI-ID Award (UM1AI100663), and LIAI institutional funds to SC.

We thank Dr. Danelle Eto and Robin Kageyama for their technical support for this work.

References

1. Crotty S. Follicular helper CD4 T cells (TFH). Annu Rev Immunol. 2011; 29:621–663. [PubMed: 21314428]
2. Haynes NM, Allen CDC, Lesley R, Ansel KM, Killeen N, Cyster JG. Role of CXCR5 and CCR7 in follicular Th cell positioning and appearance of a programmed cell death gene-1high germinal center-associated subpopulation. J Immunol. 2007; 179:5099–5108. [PubMed: 17911595]
3. Zotos D, Coquet JM, Zhang Y, Light A, D'Costa K, Kallies A, Corcoran LM, Godfrey DI, Toellner KM, Smyth MJ, Nutt SL, Tarlinton DM. IL-21 regulates germinal center B cell differentiation and proliferation through a B cell-intrinsic mechanism. J Exp Med. 2010; 207:365–378. [PubMed: 20142430]
4. O'Shea JJ, Paul WE. Mechanisms underlying lineage commitment and plasticity of helper CD4+ T cells. Science. 2010; 327:1098–1102. [PubMed: 20185720]
5. Yu D, Rao S, Tsai LM, Lee SK, He Y, Sutcliffe EL, Srivastava M, Linterman M, Zheng L, Simpson N, Ellyard JI, Parish IA, Ma CS, Li QJ, Parish CR, Mackay CR, Vinuesa CG. The transcriptional repressor Bcl-6 directs T follicular helper cell lineage commitment. Immunity. 2009; 31:457–468. [PubMed: 19631565]
6. Johnston RJ, Poholek AC, Ditoro D, Yusuf I, Eto D, Barnett B, Dent AL, Craft J, Crotty S. Bcl6 and Blimp-1 Are Reciprocal and Antagonistic Regulators of T Follicular Helper Cell Differentiation. Science. 2009; 325:1006–1010. [PubMed: 19608860]
7. Nurieva RI, Chung Y, Martinez GJ, Yang XO, Tanaka S, Matskevitch TD, Wang YH, Dong C. Bcl6 mediates the development of T follicular helper cells. Science. 2009; 325:1001–1005. [PubMed: 19628815]
8. Kroenke MA, Eto D, Locci M, Cho M, Davidson T, Haddad EK, Crotty S. Bcl6 and Maf cooperate to instruct human follicular helper CD4 T cell differentiation. J Immunol. 2012; 188:3734–3744. [PubMed: 22427637]
9. Choi YS, Kageyama R, Eto D, Escobar TC, Johnston RJ, Monticelli L, Lao C, Crotty S. ICOS receptor instructs T follicular helper cell versus effector cell differentiation via induction of the transcriptional repressor Bcl6. Immunity. 2011; 34:932–946. [PubMed: 21636296]
10. Kerfoot, Steven M.; Yaari, G.; Patel, Jaymin R.; Johnson, Kody L.; Gonzalez, David G.; Kleinstein, Steven H.; Haberman, Ann M. Germinal Center B Cell and T Follicular Helper Cell Development Initiates in the Interfollicular Zone. Immunity. 2011; 34:947–960. [PubMed: 21636295]
11. Kitano M, Moriyama S, Ando Y, Hikida M, Mori Y, Kurosaki T, Okada T. Bcl6 Protein Expression Shapes Pre-Germinal Center B Cell Dynamics and Follicular Helper T Cell Heterogeneity. Immunity. 2011; 34:961–972. [PubMed: 21636294]
12. Lu KT, Kanno Y, Cannons JL, Handon R, Bible P, Elkahloun AG, Anderson SM, Wei L, Sun H, O'Shea JJ, Schwartzberg PL. Functional and epigenetic studies reveal multistep differentiation and plasticity of in vitro-generated and in vivo-derived follicular T helper cells. Immunity. 2011; 35:622–632. [PubMed: 22018472]
13. Nakayamada S, Kanno Y, Takahashi H, Jankovic D, Lu KT, Johnson TA, Sun H-w, Vahedi G, Hakim O, Handon R, Schwartzberg PL, Hager GL, O'Shea JJ. Early Th1 Cell Differentiation Is Marked by a Tfh Cell-like Transition. Immunity. 2011; 35:919–931. [PubMed: 22195747]

14. Oestreich KJ, Mohn SE, Weinmann AS. Molecular mechanisms that control the expression and activity of Bcl-6 in T(H)1 cells to regulate flexibility with a T(FH)-like gene profile. Nat Immunol. 2012; 13:405–411. [PubMed: 22406686]
15. Johnston RJ, Choi YS, Diamond JA, Yang JA, Crotty S. STAT5 is a potent negative regulator of TFH cell differentiation. J Exp Med. 2012; 209:243–250. [PubMed: 22271576]
16. Ballesteros-Tato A, León B, Graf BA, Moquin A, Adams PS, Lund FE, Randall TD. Interleukin-2 inhibits germinal center formation by limiting T follicular helper cell differentiation. Immunity. 2012; 36:847–856. [PubMed: 22464171]
17. Vinuesa CG, Cyster JG. How T cells earn the follicular rite of passage. Immunity. 2011; 35:671–680. [PubMed: 22118524]
18. Pepper M, Pagán AJ, Igyártó BZ, Taylor JJ, Jenkins MK. Opposing signals from the bcl6 transcription factor and the interleukin-2 receptor generate T helper 1 central and effector memory cells. Immunity. 2011; 35:583–595. [PubMed: 22018468]
19. Liu X, Yan X, Zhong B, Nurieva RI, Wang A, Wang X, Martin-Orozco N, Wang Y, Chang SH, Esplugues E, Flavell RA, Tian Q, Dong C. Bcl6 expression specifies the T follicular helper cell program in vivo. J Exp Med. 2012; 209:1841–1852. [PubMed: 22987803]
20. Zaretsky AG, Taylor JJ, King IL, Marshall FA, Mohrs M, Pearce EJ. T follicular helper cells differentiate from Th2 cells in response to helminth antigens. J Exp Med. 2009; 206:991–999. [PubMed: 19380637]
21. Bluestone JA, Mackay CR, O'shea JJ, Stockinger B. The functional plasticity of T cell subsets. Nat Rev Immunol. 2009; 9:811–816. [PubMed: 19809471]
22. Murai M, Turovskaya O, Kim G, Madan R, Karp CL, Cheroutre H, Kronenberg M. Interleukin 10 acts on regulatory T cells to maintain expression of the transcription factor Foxp3 and suppressive function in mice with colitis. Nat Immunol. 2009; 10:1178–1184. [PubMed: 19783988]
23. Zhou L, Chong MMW, Littman DR. Plasticity of CD4+ T Cell Lineage Differentiation. Immunity. 2009; 30:646–655. [PubMed: 19464987]
24. Lee SK, Silva DG, Martin JL, Pratama A, Hu X, Chang PP, Walters G, Vinuesa CG. Interferon-γ Excess Leads to Pathogenic Accumulation of Follicular Helper T Cells and Germinal Centers. Immunity. 2012; 37:880–892. [PubMed: 23159227]
25. Cretney E, Xin A, Shi W, Minnich M, Masson F, Miasari M, Belz GT, Smyth GK, Busslinger M, Nutt SL, Kallies A. The transcription factors Blimp-1 and IRF4 jointly control the differentiation and function of effector regulatory T cells. Nat Immunol. 2011; 12:304–311. [PubMed: 21378976]
26. Fazilleau N, Mcheyzer-Williams LJ, Rosen H, Mcheyzer-Williams MG. The function of follicular helper T cells is regulated by the strength of T cell antigen receptor binding. Nat Immunol. 2009; 10:375–384. [PubMed: 19252493]
27. Shaffer AL, Yu X, He Y, Boldrick J, Chan EP, Staudt LM. BCL-6 represses genes that function in lymphocyte differentiation, inflammation, and cell cycle control. Immunity. 2000; 13:199–212. [PubMed: 10981963]
28. Tunyaplin C, Shaffer AL, Angelin-Duclos CD, Yu X, Staudt LM, Calame KL. Direct repression of prdm1 by Bcl-6 inhibits plasmacytic differentiation. J Immunol. 2004; 173:1158–1165. [PubMed: 15240705]
29. Oracki SA, Walker JA, Hibbs ML, Corcoran LM, Tarlinton DM. Plasma cell development and survival. Immunol Rev. 2010; 237:140–159. [PubMed: 20727034]
30. Shapiro-Shelef M, Calame K. Regulation of plasma-cell development. Nat Rev Immunol. 2005; 5:230–242. [PubMed: 15738953]
31. Belz GT, Kallies A. Effector and memory CD8+ T cell differentiation: toward a molecular understanding of fate determination. Curr Opin Immunol. 2010; 22:279–285. [PubMed: 20434894]
32. Crotty S, Johnston RJ, Schoenberger SP. Effectors and memories: Bcl-6 and Blimp-1 in T and B lymphocyte differentiation. Nat Immunol. 2010; 11:114–120. [PubMed: 20084069]
33. Weber JP, Fuhrmann F, Hutloff A. T-follicular helper cells survive as long-term memory cells. Eur J Immunol. 2012; 42:1981–1988. [PubMed: 22730020]

34. Oxenius A, Bachmann MF, Zinkernagel RM, Hengartner H. Virus-specific MHC-class II-restricted TCR-transgenic mice: effects on humoral and cellular immune responses after viral infection. Eur J Immunol. 1998; 28:390–400. [PubMed: 9485218]
35. Rutishauser RL, Martins GA, Kalachikov S, Chandele A, Parish IA, Meffre E, Jacob J, Calame K, Kaech SM. Transcriptional repressor Blimp-1 promotes CD8(+) T cell terminal differentiation and represses the acquisition of central memory T cell properties. Immunity. 2009; 31:296–308. [PubMed: 19664941]
36. McCausland MM, Yusuf I, Tran H, Ono N, Yanagi Y, Crotty S. SAP regulation of follicular helper CD4 T cell development and humoral immunity is independent of SLAM and Fyn kinase. J Immunol. 2007; 178:817–828. [PubMed: 17202343]
37. Gautier L, Cope L, Bolstad BM, Irizarry RA. affy--analysis of Affymetrix GeneChip data at the probe level. Bioinformatics. 2004; 20:307–315. [PubMed: 14960456]
38. Pavlidis P, Noble WS. Matrix2png: a utility for visualizing matrix data. Bioinformatics. 2003; 19:295–296. [PubMed: 12538257]
39. Baumjohann D, Okada T, Ansel KM. Distinct waves of BCL6 expression during T follicular helper cell development. J Immunol. 2011; 187:2089–2092. [PubMed: 21804014]
40. Nurieva RI, Chung Y, Hwang D, Yang XO, Kang HS, Ma L, Wang Y-h, Watowich SS, Jetten AM, Tian Q, Dong C. Generation of T follicular helper cells is mediated by interleukin-21 but independent of T helper 1, 2, or 17 cell lineages. Immunity. 2008; 29:138–149. [PubMed: 18599325]
41. Malek TR. The biology of interleukin-2. Annu Rev Immunol. 2008; 26:453–479. [PubMed: 18062768]
42. Deenick EK, Chan A, Ma CS, Gatto D, Schwartzberg PL, Brink R, Tangye SG. Follicular helper T cell differentiation requires continuous antigen presentation that is independent of unique B cell signaling. Immunity. 2010; 33:241–253. [PubMed: 20691615]
43. Goenka R, Barnett LG, Silver JS, O'Neill PJ, Hunter CA, Cancro MP, Laufer TM. Cutting edge: dendritic cell-restricted antigen presentation initiates the follicular helper T cell program but cannot complete ultimate effector differentiation. J Immunol. 2011; 187:1091–1095. [PubMed: 21715693]
44. Ploquin MJY, Eksmond U, Kassiotis G. B cells and TCR avidity determine distinct functions of CD4+ T cells in retroviral infection. J Immunol. 2011; 187:3321–3330. [PubMed: 21841129]
45. Poholek AC, Hansen K, Hernandez SG, Eto D, Chandele A, Weinstein JS, Dong X, Odegard JM, Kaech SM, Dent AL, Crotty S, Craft J. In vivo regulation of Bcl6 and T follicular helper cell development. J Immunol. 2010; 185:313–326. [PubMed: 20519643]
46. Kaech SM, Tan JT, Wherry EJ, Konieczny BT, Surh CD, Ahmed R. Selective expression of the interleukin 7 receptor identifies effector CD8 T cells that give rise to long-lived memory cells. Nat Immunol. 2003; 4:1191–1198. [PubMed: 14625547]
47. Marshall HD, Chandele A, Jung YW, Meng H, Poholek AC, Parish IA, Rutishauser R, Cui W, Kleinstein SH, Craft J, Kaech SM. Differential Expression of Ly6C and T-bet Distinguish Effector and Memory Th1 CD4(+) Cell Properties during Viral Infection. Immunity. 2011; 35:633–646. [PubMed: 22018471]
48. Kalia V, Sarkar S, Subramaniam S, Haining WN, Smith KA, Ahmed R. Prolonged interleukin-2Ralpha expression on virus-specific CD8+ T cells favors terminal-effector differentiation in vivo. Immunity. 2010; 32:91–103. [PubMed: 20096608]
49. Pipkin ME, Sacks JA, Cruz-Guilloty F, Lichtenheld MG, Bevan MJ, Rao A. Interleukin-2 and inflammation induce distinct transcriptional programs that promote the differentiation of effector cytolytic T cells. Immunity. 2010; 32:79–90. [PubMed: 20096607]
50. Jeannet G, Boudousquié C, Gardiol N, Kang J, Huelsken J, Held W. Essential role of the Wnt pathway effector Tcf-1 for the establishment of functional CD8 T cell memory. Proc Natl Acad Sci USA. 2010; 107:9777–9782. [PubMed: 20457902]
51. Miyazaki M, Rivera RR, Miyazaki K, Lin YC, Agata Y, Murre C. The opposing roles of the transcription factor E2A and its antagonist Id3 that orchestrate and enforce the naive fate of T cells. Nat Immunol. 2011; 12:992–1001. [PubMed: 21857655]

52. Cannarile MA, Lind NA, Rivera R, Sheridan AD, Camfield KA, Wu BB, Cheung KP, Ding Z, Goldrath AW. Transcriptional regulator Id2 mediates CD8+ T cell immunity. Nat Immunol. 2006; 7:1317–1325. [PubMed: 17086188]
53. Li J, Huston G, Swain SL. IL-7 promotes the transition of CD4 effectors to persistent memory cells. J Exp Med. 2003; 198:1807–1815. [PubMed: 14676295]
54. Kondrack RM, Harbertson J, Tan JT, McBreen ME, Surh CD, Bradley LM. Interleukin 7 regulates the survival and generation of memory CD4 cells. J Exp Med. 2003; 198:1797–1806. [PubMed: 14662907]
55. Martins GA, Cimmino L, Shapiro-Shelef M, Szabolcs M, Herron A, Magnusdottir E, Calame K. Transcriptional repressor Blimp-1 regulates T cell homeostasis and function. Nat Immunol. 2006; 7:457–465. [PubMed: 16565721]
56. King C. A fine romance: T follicular helper cells and B cells. Immunity. 2011; 34:827–829. [PubMed: 21703537]
57. Locksley RM. Nine lives: plasticity among T helper cell subsets. J Exp Med. 2009; 206:1643–1646. [PubMed: 19635860]
58. Lu KT, Kanno Y, Cannons JL, Handon R, Bible P, Elkahloun AG, Anderson SM, Wei L, Sun H, O'shea JJ, Schwartzberg PL. Functional and Epigenetic Studies Reveal Multistep Differentiation and Plasticity of In Vitro-Generated and In Vivo-Derived Follicular T Helper Cells. Immunity. 2011
59. Lüthje K, Kallies A, Shimohakamada Y, Belz GT, Light A, Tarlinton DM, Nutt SL. The development and fate of follicular helper T cells defined by an IL-21 reporter mouse. Nat Immunol. 2012; 13:491–498. [PubMed: 22466669]
60. Panzer M, Sitte S, Wirth S, Drexler I, Sparwasser T, Voehringer D. Rapid in vivo conversion of effector T cells into Th2 cells during helminth infection. J Immunol. 2012; 188:615–623. [PubMed: 22156341]
61. Wang YH, Voo KS, Liu B, Chen CY, Uygungil B, Spoede W, Bernstein JA, Huston DP, Liu YJ. A novel subset of CD4(+) T(H)2 memory/effector cells that produce inflammatory IL-17 cytokine and promote the exacerbation of chronic allergic asthma. J Exp Med. 2010; 207:2479–2491. [PubMed: 20921287]
62. Hegazy AN, Peine M, Helmstetter C, Panse I, FrOhlich A, Bergthaler A, Flatz L, Pinschewer DD, Radbruch A, Löhning M. Interferons direct Th2 cell reprogramming to generate a stable GATA-3(+)T-bet(+) cell subset with combined Th2 and Th1 cell functions. Immunity. 2010; 32:116–128. [PubMed: 20079668]
63. Mitsdoerffer M, Lee Y, Jäger A, Kim HJ, Korn T, Kolls JK, Cantor H, Bettelli E, Kuchroo VK. Proinflammatory T helper type 17 cells are effective B-cell helpers. Proceedings of the National Academy of Sciences of the United States of America. 2010; 107:14292–14297. [PubMed: 20660725]
64. Watt FM, Hogan BL. Out of Eden: stem cells and their niches. Science. 2000; 287:1427–1430. [PubMed: 10688781]
65. Oestreich KJ, Huang AC, Weinmann AS. The lineage-defining factors T-bet and Bcl-6 collaborate to regulate Th1 gene expression patterns. J Exp Med. 2011; 208:1001–1013. [PubMed: 21518797]
66. Kaech SM, Ahmed R. Memory CD8+ T cell differentiation: initial antigen encounter triggers a developmental program in naïve cells. Nat Immunol. 2001; 2:415–422. [PubMed: 11323695]
67. Mercado R, Vijh S, Allen SE, Kerksiek K, Pilip IM, Pamer EG. Early programming of T cell populations responding to bacterial infection. Journal of immunology (Baltimore, Md: 1950). 2000; 165:6833–6839.
68. Bajénoff M, Wurtz O, Guerder S. Repeated antigen exposure is necessary for the differentiation, but not the initial proliferation, of naive CD4(+) T cells. Journal of immunology. 2002; 168:1723–1729.
69. Yusuf I, Kageyama R, Monticelli L, Johnston RJ, Ditoro D, Hansen K, Barnett B, Crotty S. Germinal center T follicular helper cell IL-4 production is dependent on signaling lymphocytic activation molecule receptor (CD150). J Immunol. 2010; 185:190–202. [PubMed: 20525889]

70. Whitmire JK, Asano MS, Kaech SM, Sarkar S, Hannum LG, Shlomchik MJ, Ahmed R. Requirement of B cells for generating CD4+ T cell memory. J Immunol. 2009; 182:1868–1876. [PubMed: 19201839]
71. Zhao DM, Yu S, Zhou X, Haring JS, Held W, Badovinac VP, Harty JT, Xue HH. Constitutive activation of Wnt signaling favors generation of memory CD8 T cells. J Immunol. 2010; 184:1191–1199. [PubMed: 20026746]
72. Prlic M, Bevan MJ. Cutting edge: β-catenin is dispensable for T cell effector differentiation, memory formation, and recall responses. J Immunol. 2011; 187:1542–1546. [PubMed: 21724993]
73. Engel I, Murre C. The function of E- and Id proteins in lymphocyte development. Nat Rev Immunol. 2001; 1:193–199. [PubMed: 11905828]
74. D'Cruz LM, Rubinstein MP, Goldrath AW. Surviving the crash: transitioning from effector to memory CD8+ T cell. Semin Immunol. 2009; 21:92–98. [PubMed: 19269192]
75. Yang CY, Best JA, Knell J, Yang E, Sheridan AD, Jesionek AK, Li HS, Rivera RR, Lind KC, D'Cruz LM, Watowich SS, Murre C, Goldrath AW. The transcriptional regulators Id2 and Id3 control the formation of distinct memory CD8+ T cell subsets. Nat Immunol. 2011; 12:1221–1229. [PubMed: 22057289]
76. Ji Y, Pos Z, Rao M, Klebanoff CA, Yu Z, Sukumar M, Reger RN, Palmer DC, Borman ZA, Muranski P, Wang E, Schrump DS, Marincola FM, Restifo NP, Gattinoni L. Repression of the DNA-binding inhibitor Id3 by Blimp-1 limits the formation of memory CD8+ T cells. Nat Immunol. 2011; 12:1230–1237. [PubMed: 22057288]
77. Hand TW, Morre M, Kaech SM. Expression of IL-7 receptor alpha is necessary but not sufficient for the formation of memory CD8 T cells during viral infection. Proc Natl Acad Sci USA. 2007; 104:11730–11735. [PubMed: 17609371]
78. Duy C, Hurtz C, Shojaee S, Cerchietti L, Geng H, Swaminathan S, Klemm L, Kweon Sm, Nahar R, Braig M, Park E, Kim Y-m, Hofmann W-K, Herzog S, Jumaa H, Koeffler HP, Yu JJ, Heisterkamp N, Graeber TG, Wu H, Ye BH, Melnick A, Müschen M. BCL6 enables Ph+ acute lymphoblastic leukaemia cells to survive BCR-ABL1 kinase inhibition. Nature. 2011; 473:384–388. [PubMed: 21593872]
79. Hurtz C, Hatzi K, Cerchietti L, Braig M, Park E, Kim Y-M, Herzog S, Ramezani-Rad P, Jumaa H, Müller MC, Hofmann W-K, Hochhaus A, Ye BH, Agarwal A, Druker BJ, Shah NP, Melnick AM, Müschen M. BCL6-mediated repression of p53 is critical for leukemia stem cell survival in chronic myeloid leukemia. J Exp Med. 2011
80. Harty JT V, Badovinac P. Shaping and reshaping CD8+ T-cell memory. Nat Rev Immunol. 2008; 8:107–119. [PubMed: 18219309]
81. Katz DH, Paul WE, Goidl EA, Benacerraf B. Carrier function in anti-hapten immune responses. I. Enhancement of primary and secondary anti-hapten antibody responses by carrier preimmunization. J Exp Med. 1970; 132:261–282. [PubMed: 4101344]
82. Welsh RM, Selin LK, Szomolanyi-Tsuda E. Immunological memory to viral infections. Annu Rev Immunol. 2004; 22:711–743. [PubMed: 15032594]
83. Chevalier N, Jarrossay D, Ho E, Avery DT, Ma CS, Yu D, Sallusto F, Tangye SG, Mackay CR. CXCR5 expressing human central memory CD4 T cells and their relevance for humoral immune responses. J Immunol. 2011; 186:5556–5568. [PubMed: 21471443]
84. Bossaller L, Burger J, Draeger R, Grimbacher B, Knoth R, Plebani A, Durandy A, Baumann U, Schlesier M, Welcher AA, Peter HH, Warnatz K. ICOS deficiency is associated with a severe reduction of CXCR5+CD4 germinal center Th cells. J Immunol. 2006; 177:4927–4932. [PubMed: 16982935]

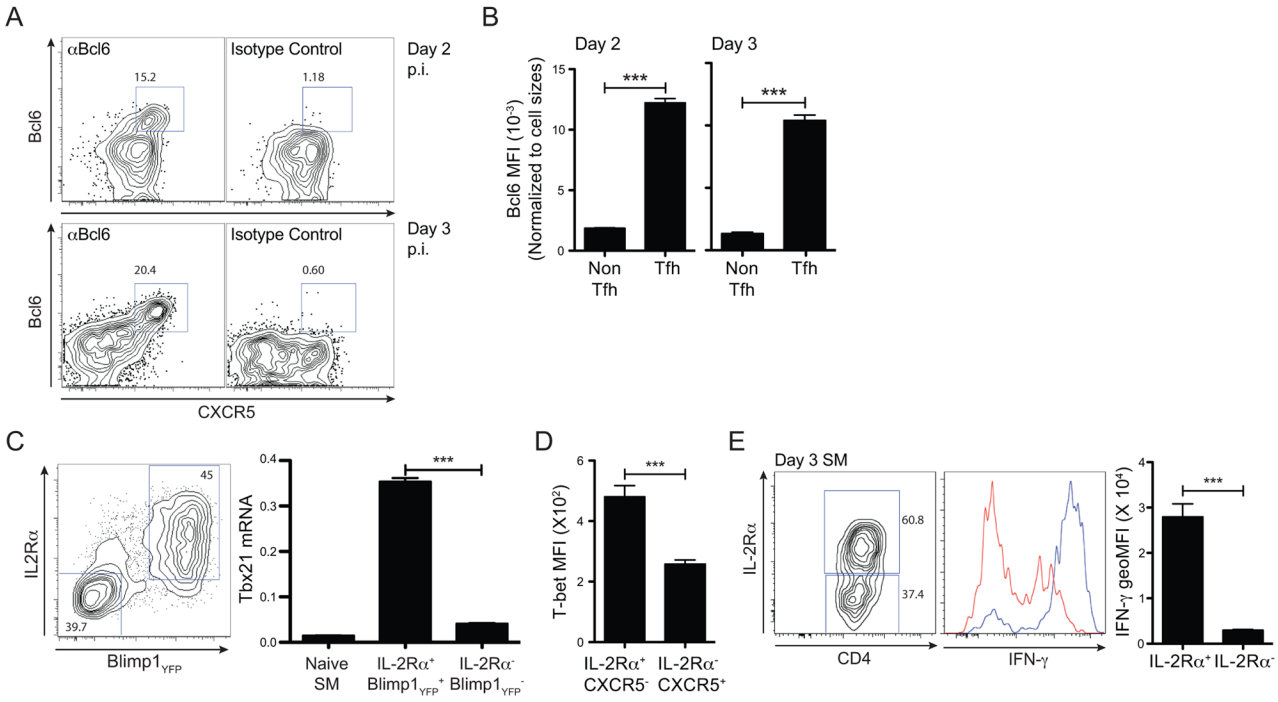

Figure 1. Early bifurcation of Tfh and Th1 differentiation pathway occurs after an acute viral infection

(A–B) Analysis for Bcl6 expression by SM CD4 T cells after LCMV infection. **(A)** Isotype control stains were included to gate Bcl6$^+$ SM cells of 2 (upper panels) and 3 (lower panels) day LCMV infected mice. **(B)** Bcl6 expression levels calculated by normalization of Bcl6 MFIs of Tfh vs. non-Tfh SM cells by cell sizes. **(C)** Naïve Blimp1-YFP SM (CD45.1$^+$) cells were transferred into B6 mice, from which IL-2Rα$^+$Blimp1$_{YFP}^+$ non-Tfh and IL-2Rα$^-$Blimp1$_{YFP}^-$Tfh cells were sorted at day 3 after LCMV infection. qPCR was conducted to measure *Tbx21* mRNA. Quantification made by fold induction of *Tbx21* over *Gapdh*. **(D–E)** Naïve SM (CD45.1$^+$) CD4 T cells were transferred into B6 (CD45.2$^+$) mice that were subsequently infected with LCMV. **(D)** T-bet MFIs calculated for IL-2Rα$^+$CXCR5$^-$ and IL-2Rα$^-$CXCR5$^+$ SM cells. **(E)** IFN-γ ICS stains conducted to detect IFN-γ production after PMA/Ionomycin stimulation. SM cells were gated based on IL-2Rα expression (left). Overlaid histograms of INF-γ of IL-2Rα$^+$ non-Tfh (blue) and IL-2Rα$^-$ (red) Tfh SM cells (middle). Quantification made by geometric MFI of IFN-γ (right). Data are representative of two independent experiments using 4–5 mice per group **(A–B and D–E)** and triplicate wells **(C)** per sample. *** $P < 0.001$. Shown as mean and SEM.

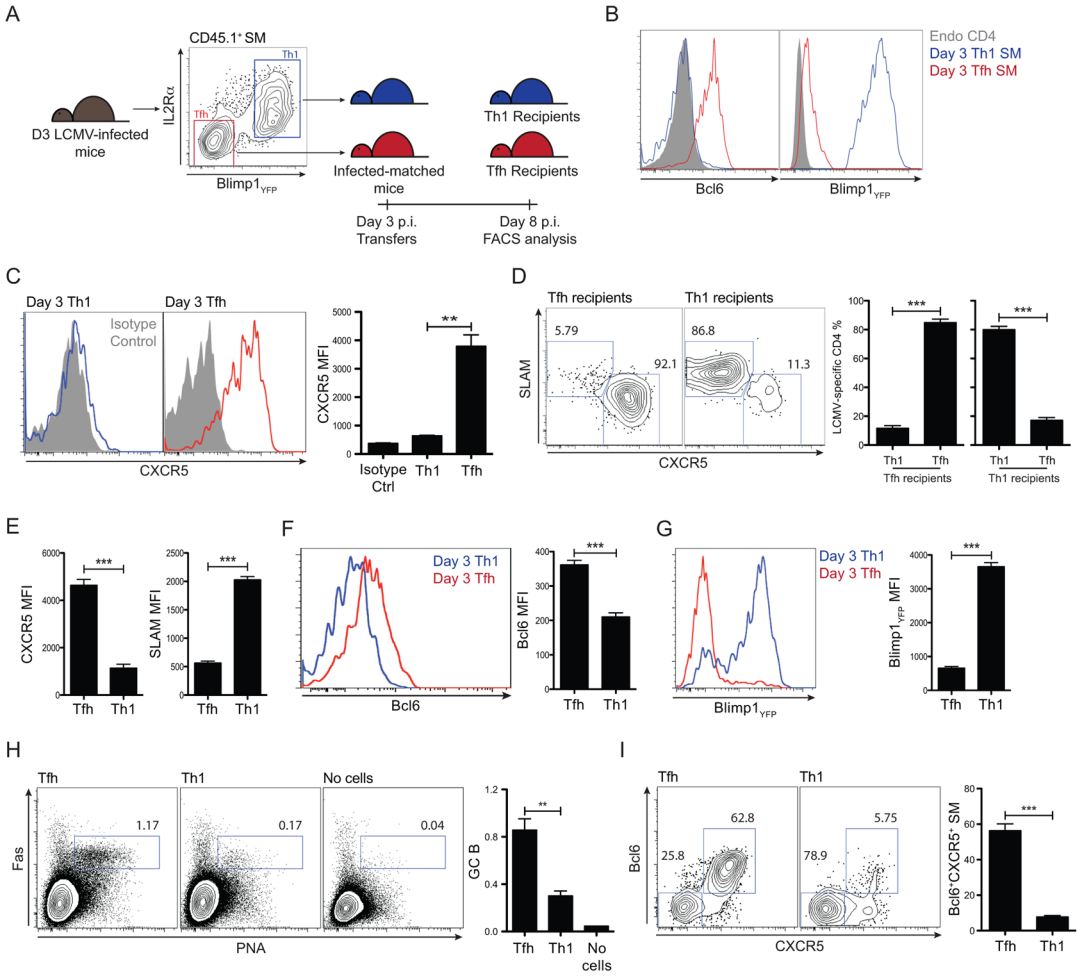

Figure 2. Tfh cells are fate determined early during an acute viral infection

(A–G) Naïve Blimp1-YFP SM (CD45.1^{+}) CD4 T cells were transferred into B6 (CD45.2^{+}) mice that were infected with LCMV. **(A)** Three days after LMCV infection, SM cells were FACS sorted into Tfh (IL-2Rα^{-}Blimp1$_{YFP}^{-}$) vs. Th1 (IL-2Rα^{+}Blimp1$_{YFP}^{+}$) SM cells. The sorted Tfh and Th1 SM cells were transferred into separate groups of infection-matched B6 mice and analyzed 5 days later. **(B)** Overlaid histograms for Bcl6 (left) and Blimp1$_{YFP}$ (right) by day 3 Th1 (blue) and Tfh (red) SM cells, with endogenous CD4 T cells (gray filled). **(C)** Overlaid histograms for CXCR5 expression by day 3 Th1 (blue) and Tfh (red) SM cells. Gray filled histograms show background stains by isotype control (rat IgG2a) mAb. Quantitation calculated as MFIs. **(D)** Representative FACS plots of splenic SM cells in Tfh (left) and Th1 (right) recipient mice 5 days after transfer. Gates indicate Th1 (SLAM^{hi}CXCR5^{lo}) and Tfh (SLAM^{lo}CXCR5^{hi}) SM cells. Relative frequencies of Th1 and Tfh SM cells calculated as percentages of respective populations among total SM cells in Th1 and Tfh recipient mice. **(E)** MFIs of CXCR5 and SLAM calculated on total SM cells in Th1 and Tfh transferred mice. Overlaid histograms of Bcl6 **(F)** and Blimp1$_{YFP}$ **(G)** expressions by SM cells in Th1 (blue) and Tfh (red) recipient mice. MFIs calculated. **(H–I)** Day 3 Tfh and Th1 cells were isolated as shown in Figure 2A, and were transferred into TCRα$^{-/-}$ mice that had been immunized with gp61-KLH 48 hours prior to adoptive cell transfer. The mice were analyzed ten days after immunization. **(H)** Shown are representative FACS plots of germinal center B cells (Fas^{+}PNA^{+}) of Tfh, Th1, or no cell transferred TCRα$^{-/-}$ splenocytes. Quantitation calculated as percent of germinal center B cells among

total B cells. **(I)** Representative FACS plots of donor cells. Gates indicate $Bcl6^{+}CXCR5^{+}$ Tfh cells. Percent of Tfh cells among total donor cells. Data are representative of two independent experiments using 5–6 mice per group. ** $P < 0.01$, *** $P < 0.001$. Shown as mean and SEM.

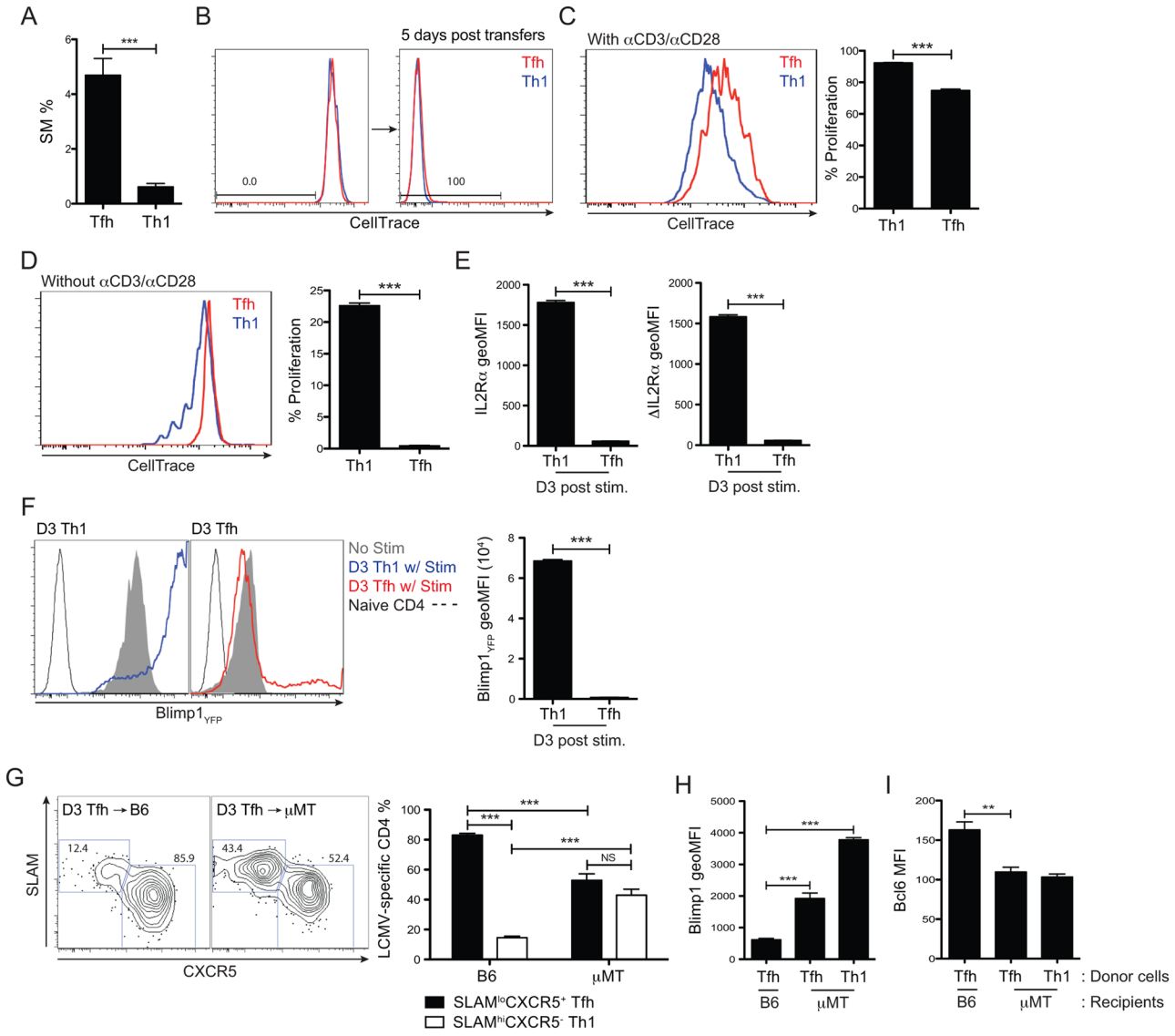

Figure 3. Fate committed Tfh cells require continuous antigenic stimulation to proliferate

(A) SM CD4 T cell expansion (% of total CD4 T cells) in spleens of Tfh vs. Th1 cell recipient mice (shown in Figure 2). **(B)** Day 3 Tfh and Th1 cells were sorted (Figure 2A), labeled with CellTrace Violet, and then transferred into infection-matched mice. Overlaid histograms show CellTrace Violet in Th1 (blue) and Tfh (red) cells before (left) and 5 days after (right) cell transfer. **(C–F)** Three days after LCMV infection, SM Tfh and Th1 cells were sorted, CellTrace Violet labeled, and then cultured for 3 days in vitro. Overlaid histograms of CellTrace Violet labeled Th1 (blue) and Tfh (red) cells 3 days after in vitro culture with **(C)** or without **(D)** αCD3/28 mAbs. **(E)** IL-2Rα levels calculated as geometric MFIs (left) and by ΔIL-2Rα geometric MFIs (right, IL-2Rα $geoMFI_{w/stim}$ – IL-2Rα $geoMFI_{w/o\ stim}$). **(F)** Overlaid histograms for $Blimp1_{YFP}$ expressions by ex vivo Th1 (blue) and Tfh (red) SM cells following αCD3/28 stimulation. Calculated as geometric MFIs. Gray filled histograms show $Blimp1_{YFP}$ levels by Th1 and Tfh cells cultured in the absence of stimulation. **(G–I)** $Bcl6^{+}CXCR5^{+}$ Tfh ($CD45.1^{+}$) cells were obtained from day 3 LCMV infected B6 mice, transferred into infection-matched B6 or B cell-deficient μMT recipient ($CD45.2^{+}$) mice, and analyzed 5 days after transfers. **(G)** Representative FACS plots of

transferred ($CD45.1^+$) cells. Gates indicate Th1 ($SLAM^{hi}CXCR5^-$) and Tfh ($SLAM^{lo}CXCR5^+$) cells. Relative frequencies of Th1 and Tfh populations calculated as % of total transferred cells. Levels of $Blimp1_{YFP}$ **(H)** and Bcl6 **(I)** expression by transferred cells in Tfh-recipient B6 and μMT mice and Th1-recipient μMT mice. Data are representative of two or more independent experiments using 5–6 mice **(A–B and G–I)** and 3–4 replicate wells **(C–F)** per group. ** $P < 0.01$, *** $P < 0.001$. Shown as mean and SEM.

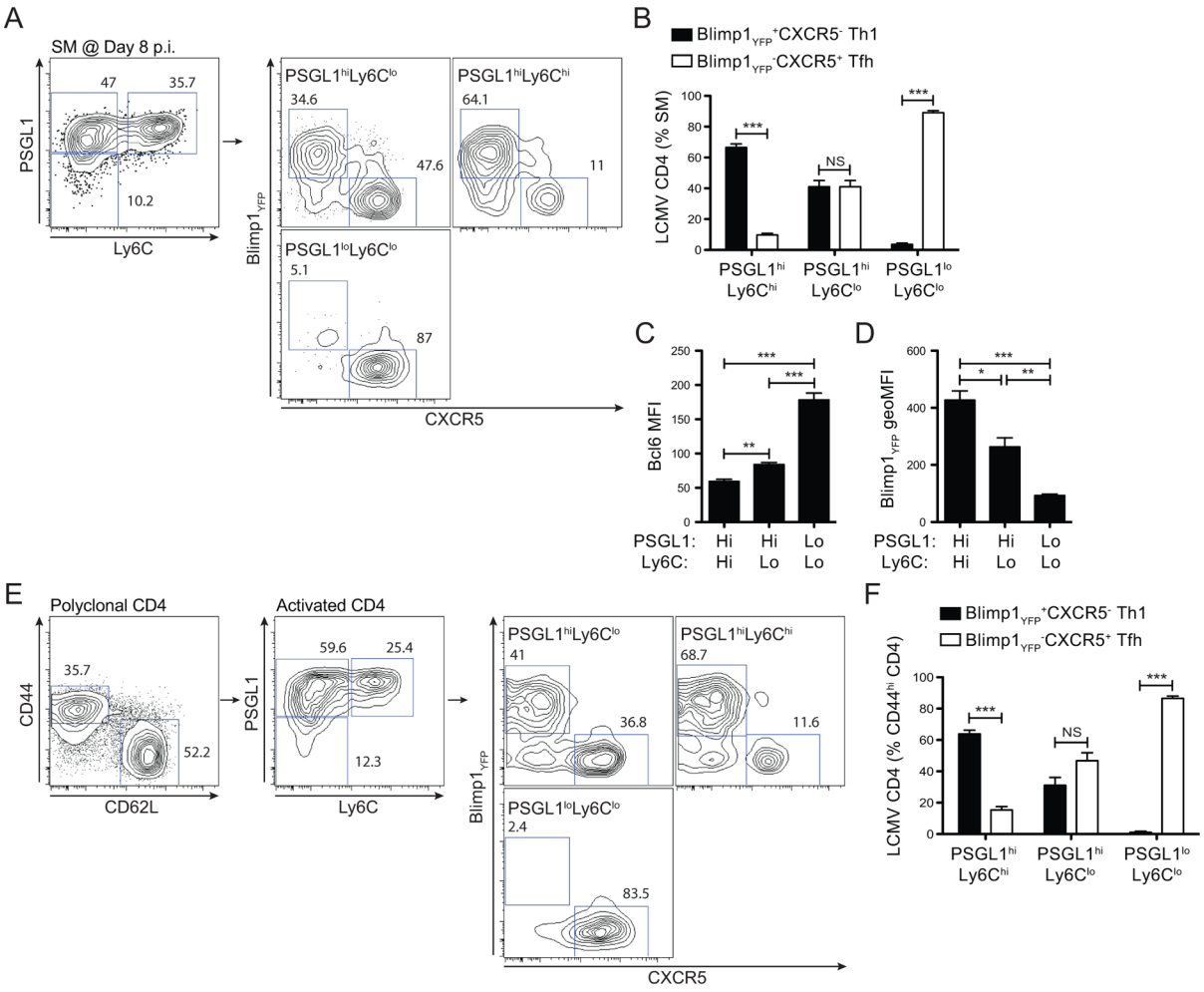

Figure 4. PSGL1^{hi}Ly6C^{lo} compartment consists of fully differentiated Tfh and Th1 cells

(A–D) LCMV-specific Blimp1-YFP SM (CD45.1^{+}) CD4 T cells were divided into three compartments (PSGL1^{hi}Ly6C^{hi}, PSGL1^{hi}Ly6C^{lo}, and PSGL1^{lo}Ly6C^{lo}) in B6 (CD45.2^{+}) mice at day 8 after infection. The three populations were further separated into Blimp1$_{YFP}$$^{+}$CXCR5^{-} Th1 and Blimp1$_{YFP}$$^{-}$CXCR5^{+} Tfh cells. **(A)** Representative FACS plots of SM cells. Gates indicate PSGL1^{hi}Ly6C^{hi}, PSGL1^{hi}Ly6C^{lo}, and PSGL1^{lo}Ly6C^{lo} SM populations (left). Blimp1$_{YFP}$ and CXCR5 expression was analyzed (right). **(B)** Percentages of Blimp1$_{YFP}$$^{+}$CXCR5^{-} non-Tfh and Blmp1$_{YFP}$$^{-}$CXCR5^{+} Tfh cells from PSGL1^{hi}Ly6C^{hi}, PSGL1^{hi}Ly6C^{lo}, and PSGL1^{lo}Ly6C^{lo} gates calculated. Bcl6 MFIs **(C)** and Blimp1$_{YFP}$ geometric MFIs **(D)** calculated. **(E–F)** Blimp1-YFP B6 mice were infected with LCMV and activated (CD44^{hi}CD62L^{-}) CD4 T cells were analyzed for PSGL1 and Ly6C expression. **(E)** Blimp1$_{YFP}$ and CXCR5 expression was further examined. **(F)** Relative frequencies of Blimp1$_{YFP}$$^{+}$CXCR5^{-} Th1 and Blimp1$_{YFP}$$^{-}$CXCR5^{+} Tfh cells. N = 3–4 mice per group. * P < 0.05, ** P < 0.01, *** P < 0.001. NS, not statistically different. Shown as mean and SEM.

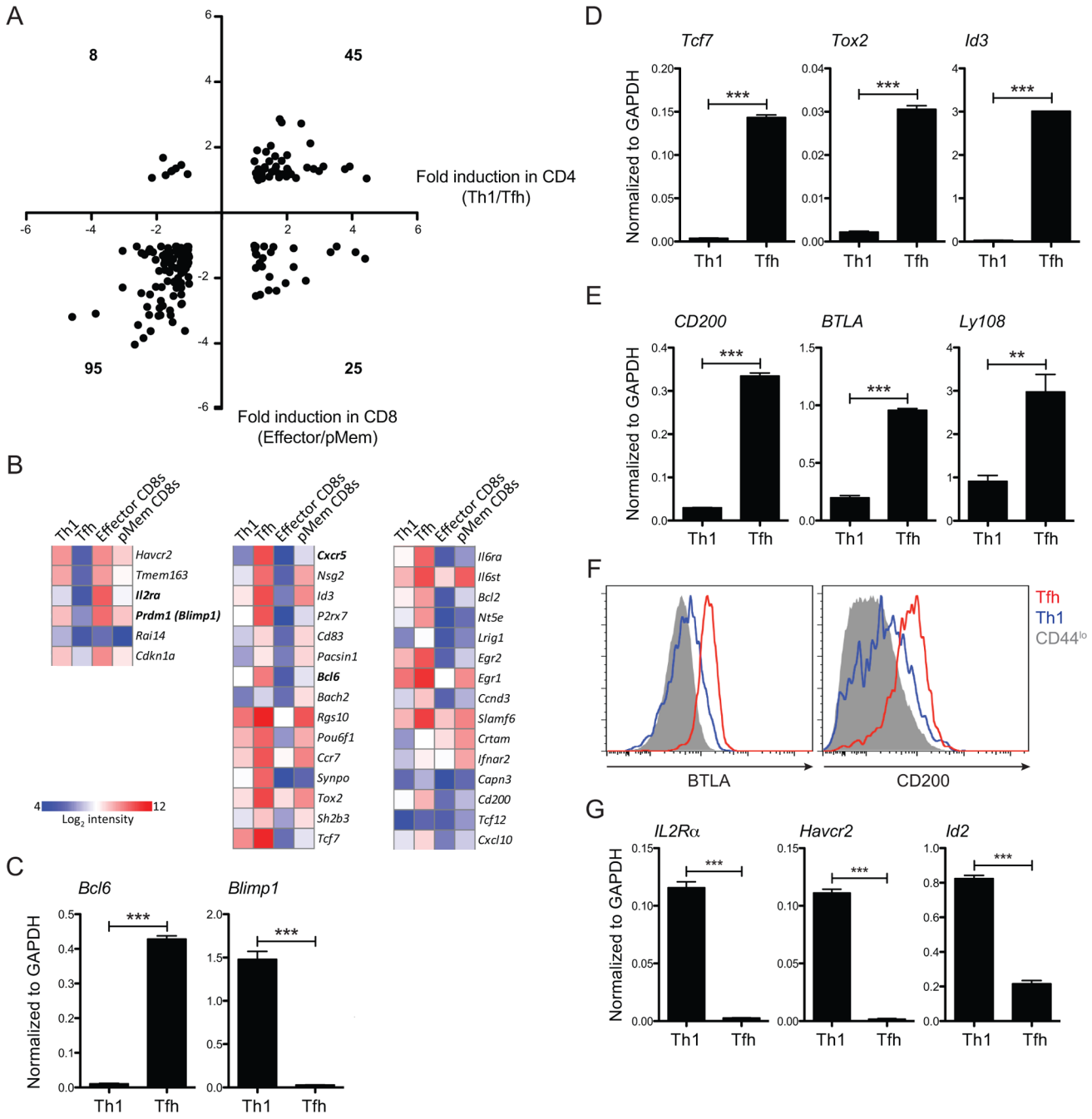

Figure 5. Early fate committed Tfh cells share a molecular signature with memory precursor CD8 T cells

Microarray data, obtained from three independent studies were normalized and analyzed (described in detail in **Materials and Methods**). **(A)** A total of 173 genes that were identified to be used commonly by both CD4 and CD8 T cells are shown in a scatter plot. Bold numbers mean number of genes in each quadrant. **(B)** Heat map of mRNA expression of 36 representative genes. **(C–E and G)** Tfh ($IL2R\alpha^{-}Blimp1_{YFP}^{-}$) and Th1 ($IL2R\alpha^{+}Blimp1_{YFP}^{+}$) cells were sorted 72 hours after LMCV infection (Figure 2A). qPCR analysis performed with isolated mRNA for analysis of relative expressions of *Bcl6* and *Blimp1* **(C)**, *Tcf7*, *Tox2*, and *Id3* **(D)**, *CD200*, *BTLA*, and *Ly108* (*Slamf6*) **(E)**, and *Il2ra*,

Havcr2, and *Id2* **(G)**. Normalized to *Gapdh*. **(F)** Surface expressions of BTLA and CD200 by Tfh (red) and Th1 (blue) cells compared to those of naïve CD4 (gray filled) cells. Data are representative of two independent experiments with 3 replicates each **(C–E and G)**. ** $P < 0.01$, *** $P < 0.001$. Shown as mean and SEM.

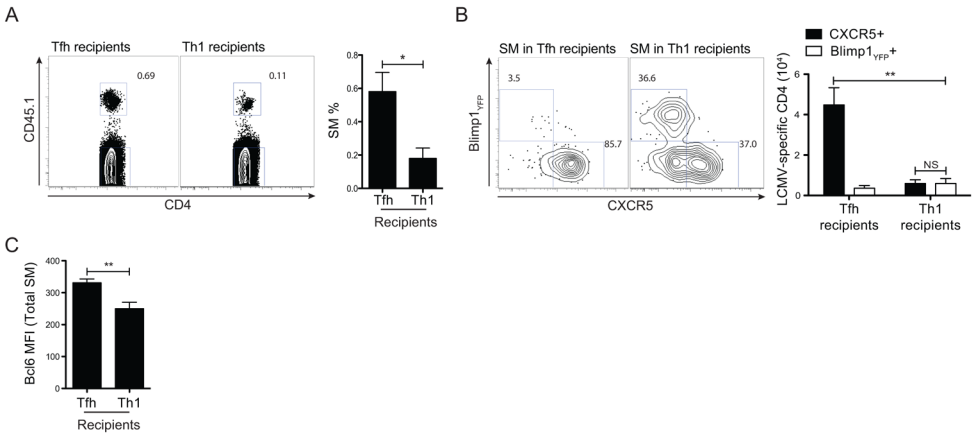

Figure 6. Fate determined Tfh cells contribute to CD4 T cell memory

(A) Day 3 Tfh (IL-2Rα^{-}Blimp1$_{YFP}^{-}$) and Th1 (IL-2Rα^{+}Blimp1$_{YFP}^{+}$) cells were sorted and transferred into separate groups of infection-matched B6 mice (Figure 2A). Tfh and Th1 recipients were analyzed 45 days after LCMV infection. Representative FACS plots for SM cells in spleens of Tfh and Th1 cell recipients. Quantifications determined as percentages of number of SM cells in total CD4 T cells. **(B)** Th1 (Blimp1$_{YFP}^{+}$CXCR5^{-}) and Tfh (Blimp1$_{YFP}^{-}$CXCR5^{+}) cells gated on total SM cells of respective recipient mice. Quantitation made as the numbers of Th1 (gray) and Tfh (black) cells in spleen. **(C)** Bcl6 MFIs of total donor cells in 45 days LCMV infected recipient mice. Data are representative of two experiments at two different memory time points (day 30 and day 45) after LCMV infection. n = 5–6 mice per group. * $P < 0.05$, ** $P < 0.01$. Shown as mean and SEM.

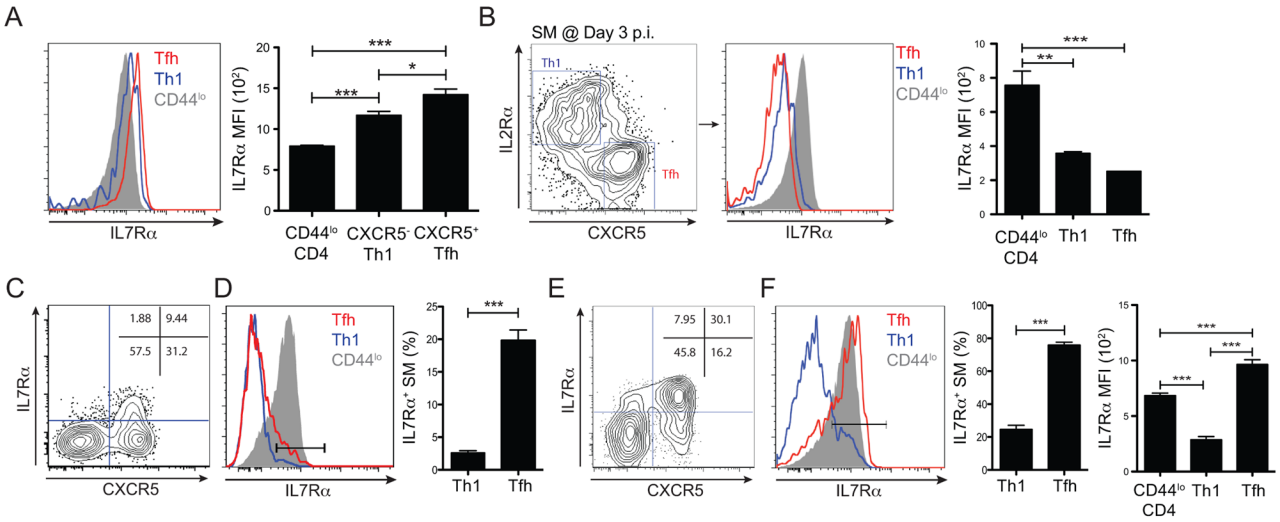

Figure 7. Tfh cells regain IL-7Rα expressions at the peak of the immune response and maintain higher expression of IL-7Rα in memory phase

(A) Overlaid histograms for IL-7Rα expression by CD44^{lo} CD4 T cells in a naïve mouse (gray filled), and Th1 (blue) and Tfh (red) cells in Th1 and Tfh recipient mice, respectively from day 45 after LCMV infected B6 mice. Quantitation calculated as MFIs. Data are representative of two experiments that were singly done at two different memory time points (day 30 and day 45) after LCMV infection**. (B)** Naïve SM (CD45.1^{+}) CD4 T cells were transferred into B6 mice that were subsequently infected with LCMV. Th1 (IL-2Rα^{+}CXCR5^{-}) and Tfh (IL-2Rα^{-}CXCR5^{+}) cells were obtained from 3 day LCMV infected spleens. IL-7Rα expression depicted by overlaid histograms (CD44^{lo} CD4 T cells in a naïve mouse, shown in gray filled; Th1 (blue) and Tfh (red) of 3 days LCMV infected mice). **(C–F)** Naive SM (CD45.1^{+}) CD4 T cells were transferred into B6 mice that were subsequently infected with LCMV. SM cells were analyzed at day 8 **(C–D)** and 11 **(E–F)** after LCMV infection. **(C)** Representative FACS plots of SM cells 8 days after LCMV infection. **(D)** Overlaid histograms for IL-7Rα expression by CD44^{lo} CD4 T cells in a naïve mouse (gray filled), and Th1 (blue) and Tfh (red) cells from LCMV infected mice at day 8. The bar indicates IL-7Rα^{hi} expressing cells. Quantitation done as IL-7Rα^{hi} % of Th1 (CXCR5^{-}) and Tfh (CXCR5^{+}) cells. **(E)** SM cells were gated by CD45.1 expression and were subsequently analyzed by IL-7Rα and CXCR5 expression. Numbers in each quadrant indicate frequencies of populations among total SM cells. **(F)** Overlaid histograms for IL-7Rα expression by CD44^{lo} naïve CD4 (gray filled) of naïve mouse, and Th1 (blue) and Tfh (red) cells from 11 days LCMV infected spleens. The bar indicates IL-7Rα expressing cells. Quantifications made as percentages of IL-7Rα expressing cells within Th1 vs. Tfh cells (middle) and total IL-7Rα MFIs (right). Data are representative of two independent experiments **(B–F)**. n = 4–6 mice per group. * P < 0.05, ** P < 0.01, *** P < 0.001. Shown as mean and SEM.

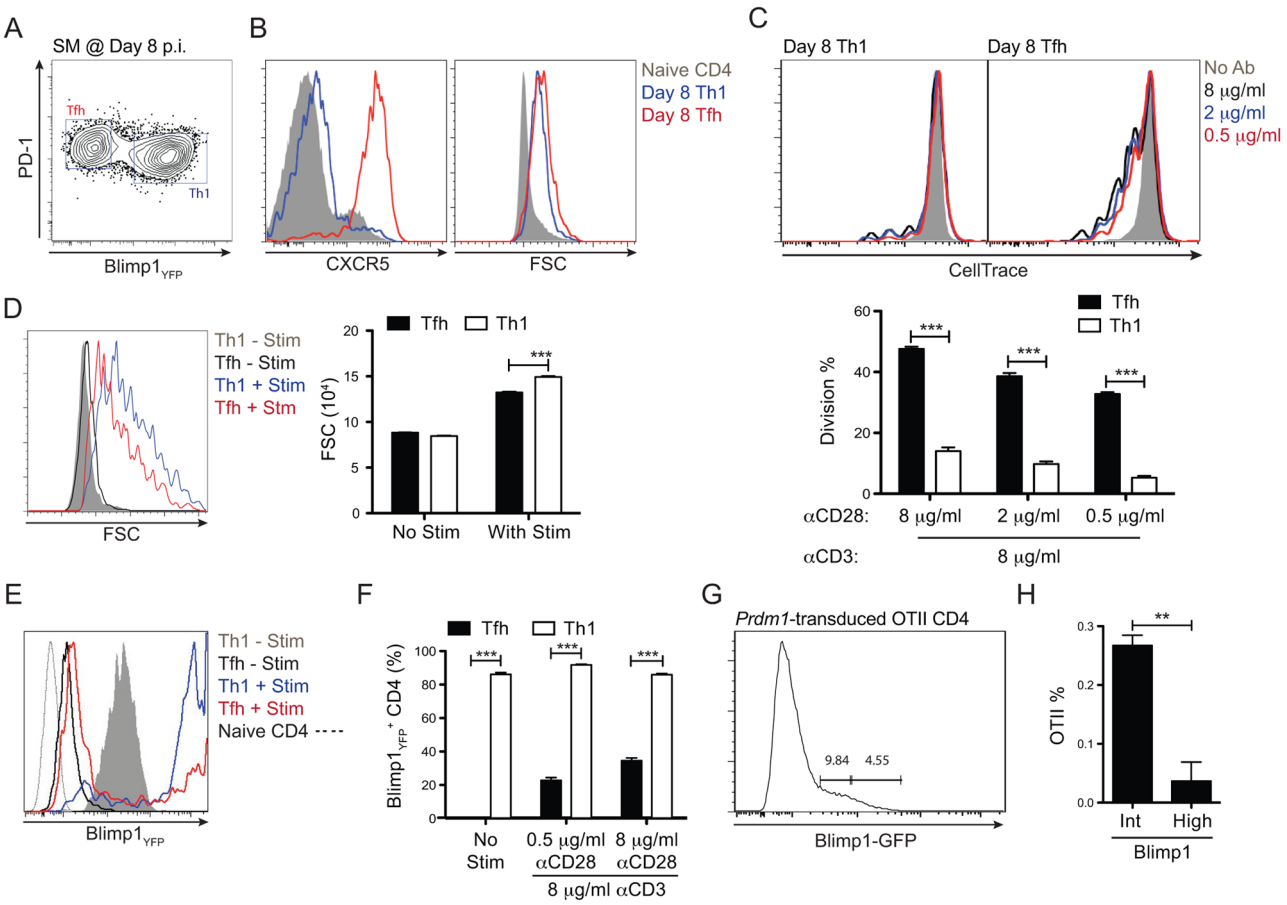

Figure 8. Tfh cells respond to antigenic re-stimulation signals

(A) Schematic diagram of Tfh (PD-1^{hi}Blimp1$_{YFP}^{-}$) and Th1 (PD-1^{int}Blimp1$_{YFP}^{+}$) SM cells sorted from day 8 LCMV infected mice. **(B)** Representative overlaid histograms for CXCR5 expression and cell size of Th1 (blue) and Tfh (red) cells. **(C)** Overlaid histograms show proliferations of Th1 (left) and Tfh (right) cells in the absence of stimulation (gray filled) or in the presence of 8 μg/ml of αCD3 mAbs with different amount of αCD28 mAbs (8 μg/ml in black; 2 μg/ml in blue, 0.5 μg/ml in red) (upper panels). Quantifications made as percentages of divided cells by Tfh (black) and Th1 (gray) cells 3 days after in vitro culture (lower panel). **(D)** Cell sizes determined by FSC of activated Tfh (red) and Th1 (blue) cells compared to those of non-activated Tfh (black) and Th1 (gray filled) cells. Quantitation made as MFIs of FSC. **(E)** Level of Blimp1$_{YFP}$ expression depicted by overlaid histograms of activated Tfh (red) and Th1 (blue) cells compared to those of non-activated Tfh (black) and Th1 (gray filled) cells. Dashed lines show background level of Blimp1$_{YFP}$ by CD44^{lo} naïve CD4 T cells in naïve mouse. **(F)** Quantitation made as percentages of Blimp1$_{YFP}$-expressing cells in indicated culture conditions. Data are representative of two or more independent experiments using 3–5 replicate wells per group. **(G–H)** OTII CD4 (CD45.1^{+}) T cells were transduced with a retroviral vector that expresses Blimp1 with GFP. **(G)** Blimp1^{int} (GFP^{int}) and Blimp1^{hi} (GFP^{hi}) expressing cells were sorted based on GFP expression (left), and transferred into B6 (CD45.2^{+}) mice. **(H)** Expansion of OTII CD4 T cells were measured 8 days after NP-OVA immunization, as % of total CD4 T cells. n = 3–4 per group. ** P < 0.01, *** P < 0.001. Shown as mean and SEM.